8

The Effect of Fillers on the Mechanical Properties of Filled Materials

8.1 TENSILE STRENGTH AND ELONGATION

Tensile strength testing is by far the most popular method of evaluating of filled materials. This can be seen from the numerous publications which analyze the subject.[1-56] The information in this section is organized to provide the following information:

- Generalized models describing tensile properties of filled materials
- The effects of different fillers on tensile properties
- Methods of improving of tensile properties

A general equation describes the effect of the volume fraction of a filler on tensile strength:

$$\sigma_c = \sigma_p(1 - a\phi_f^b + c\phi_f^d) \qquad [8.1]$$

where:

σ_c	tensile strength of composite
σ_b	tensile strength of polymer matrix
ϕ_f	volume fraction of filler
a, b, c, d	constants

Without knowing the values of these coefficients, it is not possible to predict if tensile strength of the composite increases or decreases as the volume fraction of the filler increases. It is also obvious from the form of the equation that constants can be selected to describe certain features of the filler's behavior. For example, constant "a" is usually related to stress concentration. In composites, in which the filler has very poor adhesion, a = 1.21 or a = 1.23 for non-spherical particles.[1] The constant "b" is usually assigned the arbitrary value of 0.67. Constants "c" and "d" relate to the effect of particle size. The smaller the particle size, the larger are the values of these constants. When the values of these four constants are known or approximated, it makes it possible to predict the tensile strength of various composites. Since the last term in Eq 8.1 is positive, a decrease in the particle size of the filler

should result in an increase in tensile strength. Many modifications of the above equation or its parameters (constants) are used to explain experimental data.

For low concentrations of filler, the Einstein equation usually fits experimental data:

$$\sigma_c = \sigma_p(1 + a\phi_\phi^b) \qquad [8.2]$$

In the Einstein equation, b = 1 for spherical particles at low concentration and "a" depends on the adhesion between the matrix and the filler. This equation predicts that the addition of filler increases tensile strength which was found to be not always the case, so this equation has been modified by various researchers. The Nicolais and Narkis equation[57] is a common modification in which a=1.21 and b=2/3.[3,4,8,11]

A modified Nielsen model[58] is another frequently used equation,[1,3,9,10] especially in the form proposed by Nicolais and Narkis:[57]

$$\sigma_c = \sigma_p \frac{(1-\phi_f)}{1+2.5\phi_f} \exp(B\phi_f) \qquad [8.3]$$

In this equation "B" is a parameter characterizing the interaction.

Some other equations are also in use. One is the Piggott and Leinder equation:[59]

$$\sigma_c = \lambda\sigma_p - \chi\phi_f \qquad [8.4]$$

where:

λ	stress concentration factor
χ	constant dependent on particle-matrix adhesion

which correlates well with experimental measurements made on polymer composites.

Neither of the above equations considers the filler particle as the potential week point in the composite. Instead, the above equations assume that either the matrix fails or loss of adhesion between the filler and the matrix is responsible for failure. The equation below gives the balance of stress in a composite:

$$\phi_f k\sigma^e + (1-\phi_f) < \sigma^m = \sigma^e \qquad [8.5]$$

where:

k	proportionality constant for stress transfer
σ^e	external load
$<\sigma^m>$	average stress in the matrix
$\phi_f k\sigma^e$	load carried by the filler

Properties of filler can be compared with the stress applied to the filler particle.[5]

In fiber-filled composites, the Kelly and Tyson equation[60] can be used to estimate the effect of properties of fiber on the load bearing properties of a composite:

$$\sigma_c = \eta_o \frac{\sigma_f L_f}{2L_c} \phi_f + (1-\phi_f)\sigma_p \quad [8.6]$$

where:

η_b	fiber orientation efficiency factor
σ_f	tensile strength of fiber
L_f	mean fiber length
L_c	critical fiber length

In this equation, the mechanical properties, length, and orientation of the fiber are accounted for. In fiber-filled composites, mechanical properties depend also on fiber-fiber proximity:

$$N = A \phi_f L_f / d \quad [8.7]$$

where:

N	the average number of virtual touches per fiber
A	coefficient (=$8/\pi^2$ for random in-plane orientation)
d	fiber diameter

The results of tensile testing are frequently presented in the form of stress-strain curves or are related to the tensile modulus as given by equation:

$$E = \frac{\sigma}{\varepsilon} = \frac{F / A}{(l_1 - l_o)/l_o} \quad [8.8]$$

where:

σ	tensile stress
ε	tensile strain
F	tensile force
A	original cross-sectional area
l_o	original length
l_1	final length

The results of experimental studies summarized in the Table 8.1 show the potential effect of different fillers on tensile properties of filled materials. The first column gives a list of pairs of polymer and filler for which data on the tensile properties are available in the literature. For each pair, the actual concentration of filler used in the system is given in column 2. Either the specific concentrations are given (e.g., 10 & 20) or the concentration range (e.g., 5–50) if more than two concentrations of filler were tested. The concentration is given in weight percent unless otherwise specified. For the concentration of filler given in the second column, the respective changes of the tensile strength are given in the third column. The values in the third column are percentage of increase (plus sign) or decrease (minus sign) of the tensile strength of the filled material relative to the unfilled polymer. In the last column, short comments are given either to indicate what might have caused the observed changes (e.g., interaction, particle size, modification, etc.) or to give data on relative change of elongation of these samples.

Table 8.1. Effect of fillers on tensile properties of filled materials

Filler/polymer	Conc. range, wt%	Tensile Strength (+) decrease (-), %	Refs.	Comments
PARTICULATE, INORGANIC FILLERS				
Alumino-silicate				
PVAc	10.5%	0−+35	45	decreases with interaction increasing
Aluminum hydroxide				
chloroprene	10 & 20	+11 & +13	61	
epichlorohydrin	10 & 20	-37 & -41	61	
epoxy	5−50	-15−-36	17	elongation change: -9−-82
Antimony trioxide				
EEA	4 & 8	no effect	62	
EVA	4 & 8	no effect	62	
PE	4 & 8	no effect	62	
Barium ferrite				
natural rubber	5 & 10	-8 & -1	40	
Calcite				
PVAc	10.5%	+2−+13	45	depending on particle size
Calcium carbonate				
PE	2−25 vol%	+50−+10	10	phosphate modified
PE	2−10 vol%	-5−-50	10	not modified
PVAc	5−20	+70−+75	1	size 3.6 μm, elongation decreases
PVAc	5−20	+50−+58	1	size 5.2 μm, elongation decreases
PVAc	5−20	+40−0	1	size 16.8 μm, elongation decreases
PVAc	5−20	+55−+72	1	size 3.6 μm, stearic acid coated
PP	10−40	-5−-21	28	size 18 μm, elong. const for 10-20%
PP	5−30 vol%	-30−-45	38	compression molding, no orientation
PP	5−30 vol%	0−+20	38	injection molding, particles oriented
PP	5−30 vol%	-30−-40	53	
Clay				
EPDM	10−35	-1−-10	34	
Copper				
PA11	5−55	-10−+7	26	
Hydroxyapatite				
polyurethane	57	-45/+25	21	untreated/treated with isocyanate
Glass beads				
epoxy	10−40 vol%	-25−-60	5	no adhesion
epoxy	20−40 vol%	no effect	5	good adhesion
PA	5−40 vol%	-15−+22	8	increase only at 40 vol%
POM	10−30	-15−-40	6	
POM	24 vol%	-43−-47	4	particle size in range 7÷36 μm
PP	10−50 vol%	-11−-46	8	debonding stress; no treatment
PS	5−25 vol%	-5−-15	5	poor adhesion
PS	3−10 vol%	+5−+15	5	good adhesion
Magnesium carbonate				
LCP	20−60	+7−+30	29	elongation rapidly reduced
Magnesium hydroxide				
PEK	65	-15	63	
PP	10−50	-1−-23	64	
Mica				
PA66	20−40	-13−+27	50	increases as particle size decreases
PBT	15−40	+12−+65	50	increases with concentration
PP	5−22 vol%	+14−-7	9	no surface treatment, elongation decr.
PP	5−22 vol%	+18−+14	9	8 wt% acrylic acid treatment
Miconite				
PP	10−60	+100−+150	43	hydrated K-Mg aluminosilicate (3 μm)
Nanoparticles				
epoxy	2−24	+60−+1800	56	montmorillonite; layered composite

Filler/polymer	Conc. range, wt%	Tensile Strength (+) decrease (-), %	Refs.	Comments
Silica, fumed				
PDMS	30−50	+5−+40	65	increases as particle size decreases
Silica, precipitated				
EPM	50	+500−+700	37	depending on surface treatment
Talc				
PE	2−10	+15−+80	19,25	
PP	40	+25−+44	33	depending on phosphate coating
PP	5−30 vol%	-20−-25	38	compression molding, no orientation
PP	5−30 vol %	0−+80	38	injection molding, filler oriented
PP	5−30 vol%	-25−-36	53	
Wollastonite				
LCP	20−60	+5−+15	29	elongation rapidly reduced
PA66	15−35	-19−-25	13	used in combination with glass fiber
FIBROUS FILLERS				
Aramid fiber				
fluoroelastomer	10	+260	66	
Carbon fiber				
PP	60	+4−+23	31	depending on surface treatment
Glass fiber				
ABS	30	+40	12	
LCP	20÷60	+15−+40	29	elongation rapidly reduced
PA6	50	+100	12	
PA66	30	+100	12	
PAI	30	+54	12	
PBT	30	+75	12	
PE	30	+60−+185	12	
PEK	2−7	+105	23	
PEK	10−22 vol%	+50−+90	7	long glass fiber
PEEK	30	+75	12	
PES	30	+55	12	
POM	10−30	+25−+75	6	
PP	2−7	+30−+100	7	long glass fiber
PP	30	+50	12	
PP	30	+90	24	
PSU	30	+67	12	
Polyamide fiber				
natural rubber	5−15	-40−-64	15	elongation decreases -23 to -86
ORGANIC & RECYCLED FILLERS				
Carbon black				
EPDM	10−60	+60−+370	16	elongation change: 0 to -22
fluoroelastomer	20	+200	66	elongation increase by 100%
natural rubber	20−100	+40−+100	2	elongation change: -30 to -70%
Cellulose				
natural rubber	5−25	+35−+55	18	
Fly ash				
PE	10−50	+50−+150	35	small particles
PE	10−40	-15−+20	35	large particles
Lignin				
PE	22−72 vol%	-60−-93	22	elongation also rapidly decreases
PU foam, ground				
natural rubber	20−80	-20−+60	2,30	increase peak around 30 phr
Wood flour				
PP	20−50	-2−+10	3	elongation rapidly decreasing

The data in Table 8.1 shows how the tensile strength of composite can be improved. The following factors contribute to the improvement of tensile strength:

- Particle size (nanoparticles, carbon black, and fumed silica are examples of small particles which typically contribute to an increase in tensile strength; compare the effect of particle size on PVAc adhesive properties where different sizes of calcium carbonate were used)
- Particle shape (an aspect ratio increase in a certain range improves tensile properties; see examples for fibrous fillers and mica)
- Interaction with the matrix (untreated calcium carbonate in PE decreases tensile strength but after phosphate modification tensile strength is increased; glass beads may decrease or increase tensile strength depending on their interfacial adhesion; mica and talc give a similar effect in PP; polyamide fiber does not reinforce natural rubber because of its lack of interaction)
- Concentration (the relationship of tensile strength is not a linear function of concentration; there is a certain critical concentration above which a further increase in filler's concentration decreases tensile strength)
- Proper choice of pair filler-matrix (there should be interaction between the filler and the matrix; some combinations produce adverse results; there are cases (see alumino-silicate with PVAc) where an increased interaction reduces tensile strength due to increasing material stiffness)

Figure 8.1 illustrates the effect that the shape of a particle has on tensile properties.[6] Both relationships are linear with volume fraction of filler but they point out at different directions. The experimental data for glass beads fit Einstein's model, Eq 8.2, with a=-1.72 and b=1. The negative value of coefficient "a" indicates that the presence of glass beads has a weakening effect on the composite due to debonding. Weak adhesion and debonding reduce the volume fraction of the composite which can carry the applied load. The glass fiber data follow Kelly and Tyson model, Eq 8.6. It was calculated from the model that the fiber orientation efficiency factor is 0.3. This factor is larger than the value of 0.2 which is generally used for randomly oriented fibers. The higher value is a result of the test specimens being prepared by injection molding which tends to orient the fibers.

Figure 8.2 shows the effect of particle spacing on the tensile properties of a glass bead filled composite. Glass beads addition typically decreases the tensile strength properties of a composite. An increase in interparticle spacing contributes to the increased tensile strength of the composite.[4]

The elongation is usually inversely proportional to tensile strength which means that increasing the tensile strength of filled material usually contributes to a decrease in elongation. Table 8.1 reports two cases (EPDM and fluoropolymer reinforced with carbon black) which are different. In the first case (EPDM), elongation remains constant over a certain range of carbon black. At the second case (fluoropolymer) both tensile and elongation are increased when fillers are added.

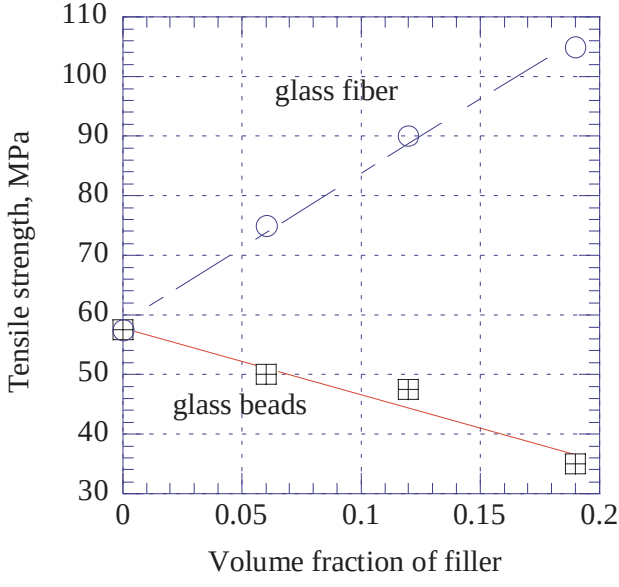

Figure 8.1. Tensile strength of POM filled with glass fibers and glass beads. [Adapted, by permission, from Hashemi S, Gilbride M T, Hodgkinson J, *J. Mat. Sci.*, **31**, No.19, 1996, 5017-25.]

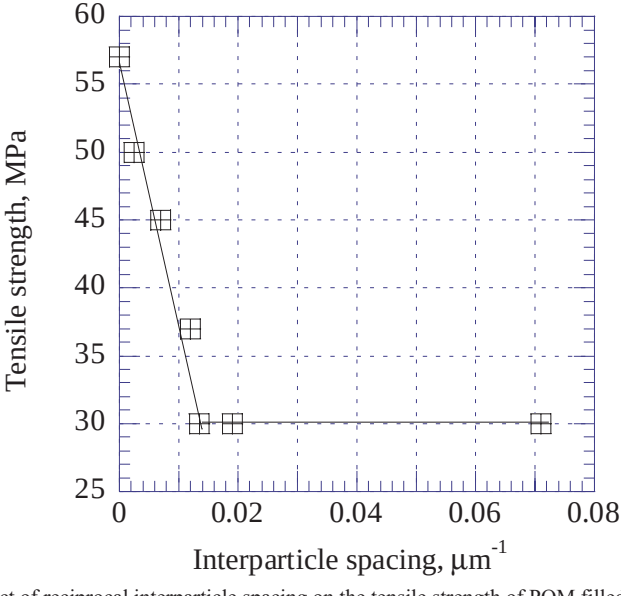

Figure 8.2. The effect of reciprocal interparticle spacing on the tensile strength of POM filled with glass beads. [Adapted, by permission, from Hashemi S, Din K J, Low P, *Polym. Engng. Sci*., **36**, No.13, 1996, 1807-20.]

Such properties can be obtained with small, interacting particles which contribute to a physical crosslinking of a relatively weak matrix. But in most cases, a reduction of elongation is an expected result of reinforcement.

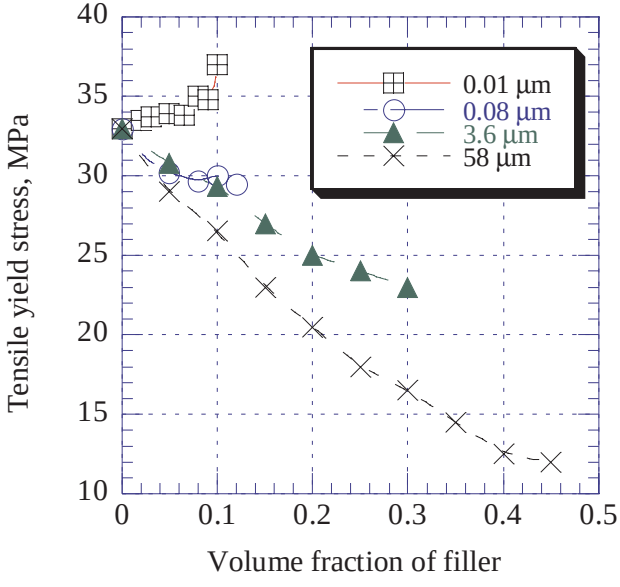

Figure 8.3. Tensile yield stress of particulate filled PP vs. filler content. [Adapted, by permission, from Voros G, Pukanszky, *J. Mat. Sci*., **30**, No.16, 1995, 4171-8.]

8.2 TENSILE YIELD STRESS

Tensile yield stress gives additional information on filler-matrix interactions and consequently it is one of the preferred methods of composite testing.[5,33,53,67-77] Figure 8.3 shows that the particle size affects yield stress of PP composites.[67] Only when filler particles become very small does the yield stress value increase as the concentration increases. The smaller the particle size the higher the value of tensile yield stress. The three largest particles are $CaCO_3$ and the smallest one is silica. Thus, yield stress behavior not only depends on particle size but also on the interaction with the matrix. If the matrix is deficient in the smallest particles of $CaCO_3$ the yield stress decreases. The stress which initiates yielding can be expressed by the equation:

$$\sigma_y = \sigma_{y0}[1-\phi_f / (1-\phi_f < \sigma^\infty >_f / \sigma^e)] \qquad [8.9]$$

where:

σ_y	external stress initiating yielding
σ_{y0}	yield stress of matrix
ϕ_f	volume fraction of filler
$<\sigma^\infty>_f$	stress inside filler particle placed into infinite matrix
σ^e	external stress
$<\sigma^\infty>_f/\sigma^e$	= k, dimensionless quantity

This equation can be rearranged into:

$$\frac{1-\phi_f}{\sigma_y} = \frac{1}{\sigma_{y0}} - \frac{k}{\sigma_{y0}}\phi_f \qquad [8.10]$$

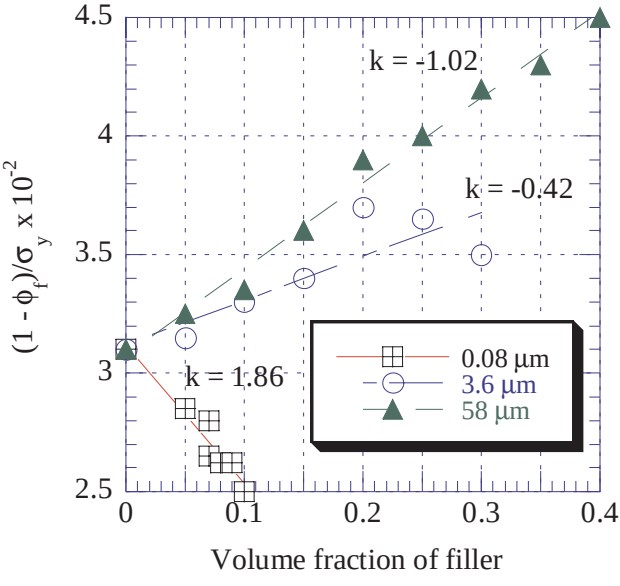

Figure 8.4. Plot of Eq 8.10. [Adapted, by permission, from Voros G, Pukanszky, *J. Mat. Sci*., **30**, No.16, 1995, 4171-8.]

Plotting $(1-\phi_f)\sigma_y$ versus ϕ_f should give straight lines with an intercept at $1/\sigma_{y0}$ and a slope of k/σ_{y0}. Figure 8.4 shows this relationship for PP/$CaCO_3$ composites from Figure 8.3. The three lines show the strong dependence of factor k on particle size. The studies were conducted for PP, PVC and LDPE.[67] Factor k depends also on the polymer used with the same fillers indicating further that the value of factor k (and yield stress) depends on polymer-filler interaction.

Figure 8.5 compares tensile yield stress for PP with two fillers.[53] In both cases, tensile yield stress decreases significantly as filler concentration increases. At higher concentrations of talc (values above 0.15 are not plotted on Figure 8.5), the composite breaks without yielding. The difference is explained by the crystallization behavior of polypropylene on the filler surface which changes the mechanical properties of composite. This shows that an additional parameter (the orientation of the polymer) may play a role in tensile yield stress behavior.

If there is perfect adhesion (no debonding), tensile yield stress increases as the concentration of the filler increases (Figure 8.6).[5] Filler particle size is also important. As the particle size of the filler decreases, the curves become more steep and the yield stress increases along with concentration increasing.

Figures 8.7 and 8.8 show applications in which various fillers increase tensile yield stress as their concentration increases. There is a linear increase in tensile yield stress (Figure 8.7) due to a strong interfacial bonding between the carbon fiber and the matrix.[75] The presence of a coupling agent increases adhesion and this is re-

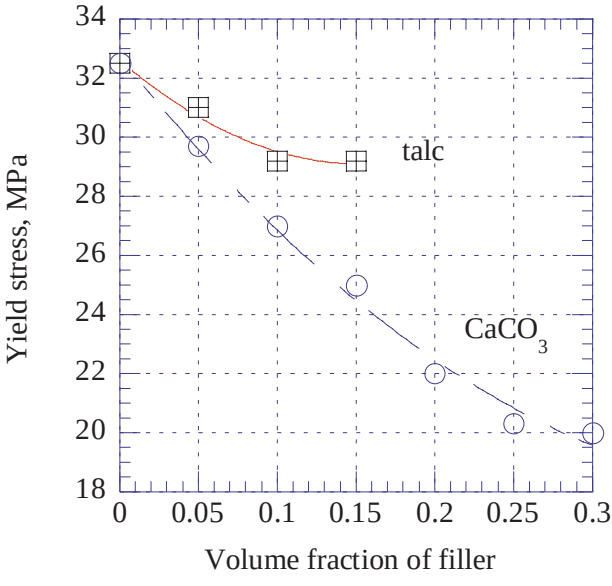

Figure 8.5. Tensile yield stress versus volume fraction of calcium carbonate and talc. [Adapted, by permission, from Pukanszky B, Belina K, Rockenbauer A, Maurer F H J, *Composites*, **25**, No.3, 1994, 205-14.]

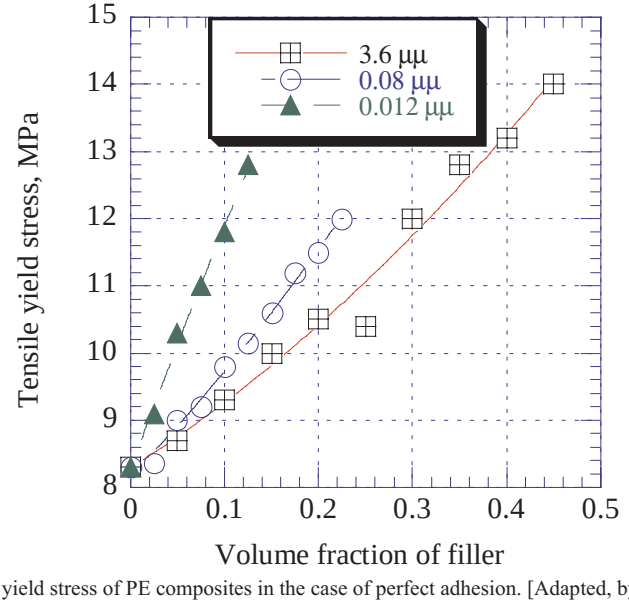

Figure 8.6. Tensile yield stress of PE composites in the case of perfect adhesion. [Adapted, by permission, from Pukanszky B, Voros G, *Polym. Composites*, **17**, No.3, 1996, 384-92.]

sponsible for the behavior presented in Figure 8.8.[73] Without a coupling agent the same composite has a tensile strength substantially lower than its yield stress.

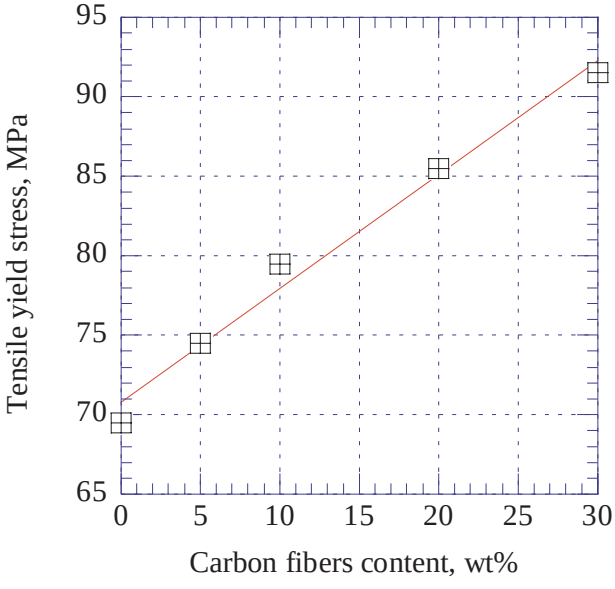

Figure 8.7. Tensile yield stress as a function of carbon fiber concentration in polycarbonate. [Adapted, by permission, from Zihlif A M, Di Liello V, Martuscelli E, Ragosta G, *Int. J. Polym. Mat*., **29**, Nos.3-4, 1995, 211-20.]

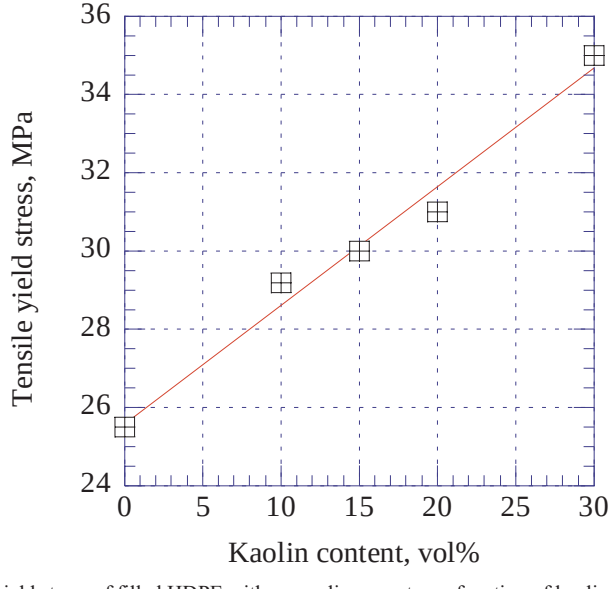

Figure 8.8. Tensile yield stress of filled HDPE with a coupling agent as a function of kaolin concentration. [Adapted, by permission, from Savadori A, Scapin M, Walter R, *Macromol. Symp*., **108**, 1996, 183-202.]

Calcium carbonate which is the most frequently used filler in PVC, decreases tensile yield stress (Figure 8.9).[71] There is good interaction and adhesion between

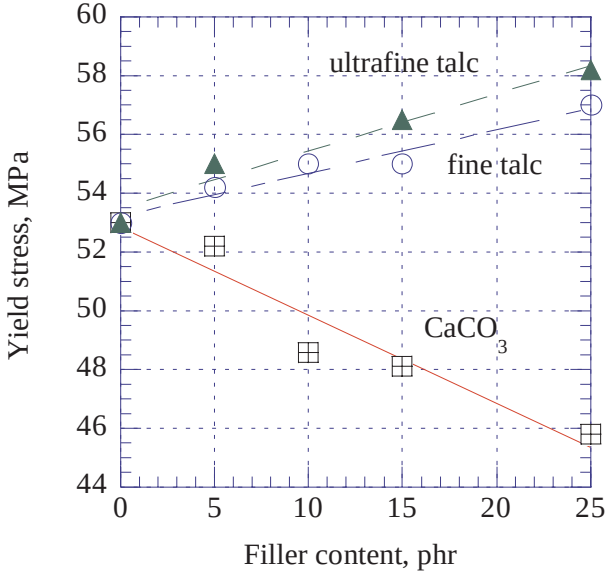

Figure 8.9. Tensile yield stress of PVC vs. filler loading. [Adapted, by permission, from Wiebking H E, Antec 95. Volume III. Conference proceedings, Boston, Ma., 7th-11th May 1995, 4112-6.]

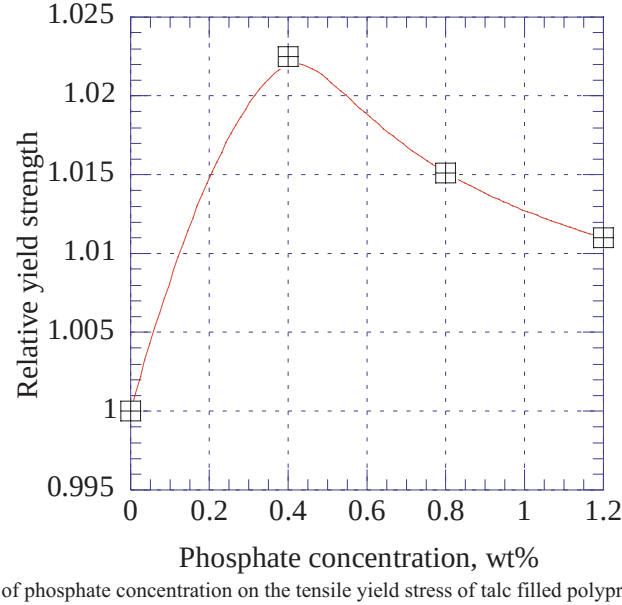

Figure 8.10. Effect of phosphate concentration on the tensile yield stress of talc filled polypropylene. [Adapted, by permission, from Liu Z, Gilbert M, *J. Appl. Polym. Sci.*, **59**, No.7, 1996, 1087-98.]

talc and PVC and the composite has a high tensile yield stress. Particle size is a less important factor.

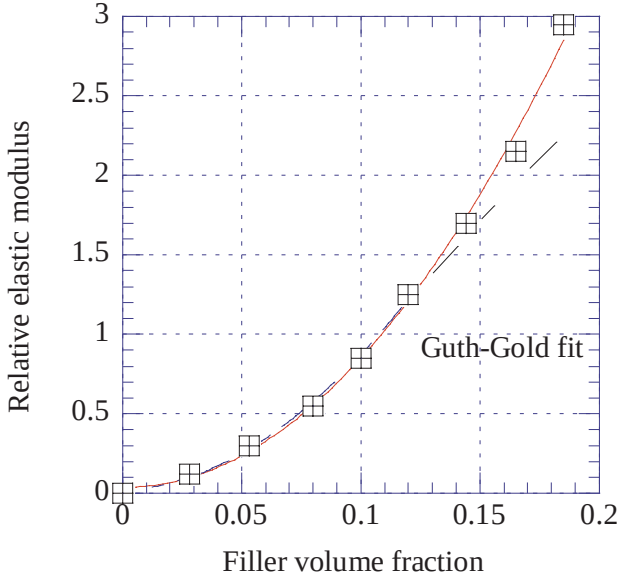

Figure 8.11. Comparison of the prediction of the Guth-Gold equation with experimental data for N330-filled SBR. [Adapted, by permission, from Wang M-J, Wolff S, Tan E-H, *Rubb. Chem. Technol*., **66**, No.2, 1993, 178-95.]

Tensile yield strength can be improved by surface treatment of filler (Figure 8.10).[33] The coating influenced the crystallinity by contributing to nucleation. This, in turn, changes the mechanical properties of the composite. At smaller additions of phosphate, polypropylene has much higher crystallinity. A concentration of phosphate below 0.5 wt% gives the greatest tensile yield stress improvement.

In summary, tensile yield stress depends on filler particle size, concentration and on the interaction between the matrix and the filler. There are various means of improving tensile yield stress through the proper selection of filler for a particular polymers and through the surface modification of filler.

8.3 ELASTIC MODULUS

Elastic modulus or Young modulus are frequently used to characterize filled systems.[22,33,53,72,75,77-90] Einstein's viscosity equation modified by Guth and Gold predicts:

$$E = E_o(1 + 2.5\phi + 14.1\phi^2) \qquad [8.11]$$

predicts that elastic modulus, E, increases as the filler concentration, ϕ, increases. Its prediction is quite precise at low concentrations (Figure 8.11).[78] At high filler concentrations the rate of change of elastic modulus deviates from that predicted by the equation.

Materials filled with rigid particles follow closely the predicted growth in elastic modulus as filler concentration increases. Many examples can be found in the

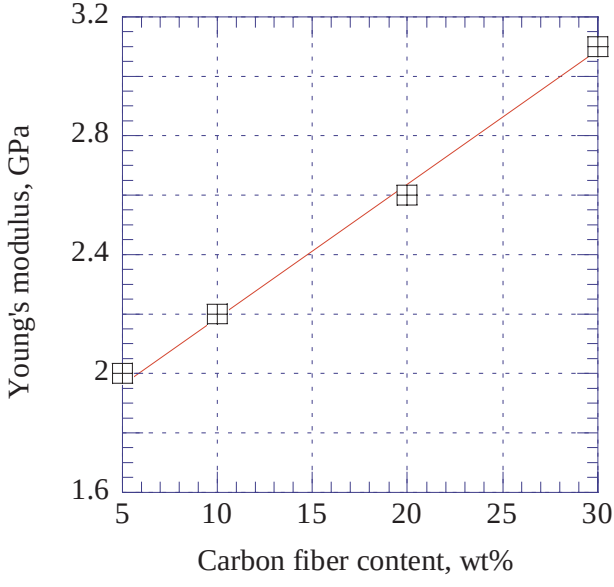

Figure 8.12. Tensile Young's modulus of a copolycarbonate composite as a function of carbon fiber concentration. [Adapted, by permission, from Zihlif A M, Di Liello V, Martuscelli E, Ragosta G, *Int. J. Polym. Mat.*, **29**, Nos.3-4, 1995, 211-20.]

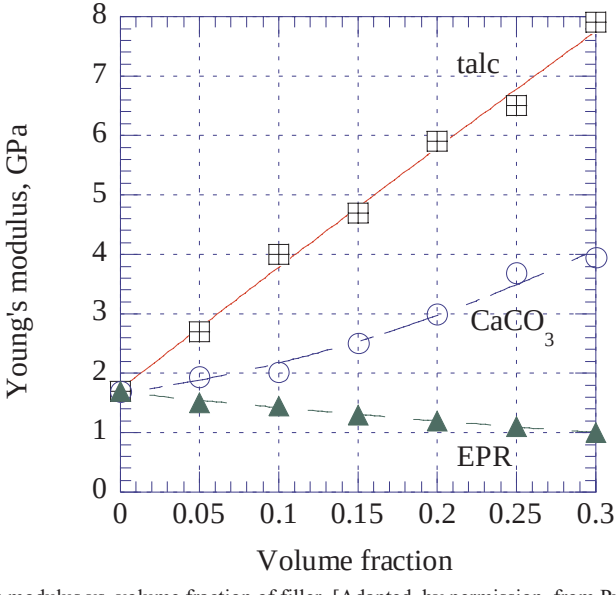

Figure 8.13. Young's modulus vs. volume fraction of filler. [Adapted, by permission, from Pukanszky B, Maurer F H J, Boode J W, *Polym. Engng. Sci.*, **35**, No.24, 1995, 1962-71.]

literature to confirm this prediction. Figure 8.12 shows the relationship for polycarbonate filled with carbon fibers.[75] The stiffness of the material increases linearly as

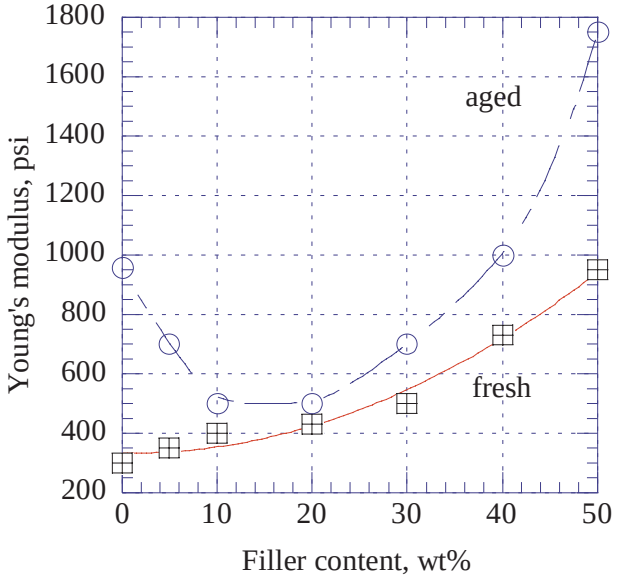

Figure 8.14. Young's moduli for fresh and aged silicone elastomer containing ZnO. [Adapted, by permission, from Yang A C M, *Polymer*, **35**, No.15, 1994, 3206-11.]

carbon fiber concentration increases and the material becomes increasingly brittle due to the nature of the fibers.

Figure 8.13 shows relationships for 3 materials.[72] Both calcium carbonate and talc generate an increased modulus whereas the addition of an elastic material such as EPR slightly reduces the value of Young's modulus. The theory predicts this because filler is composed of rigid particles, for example, calcium carbonate or talc. Better adhesion and plate like structure of talc are instrumental in rapid increase of Young's modulus.

In most of the experimental cases,[9,15,32,53,80-82,84-90] Young's modulus increases as predicted by Eq 8.11. The decrease of Young's modulus was noted when EPR[72] and lignin[22] were added.

There are other applications of elastic modulus. One can be to determine the adhesion between a filler and the matrix. To do this, elastic modulus is measured twice: once on the fresh sample and again on a sample which has been prestressed to specific strain. The decrease in Young's modulus is a measure of debonding.[83,91] Other means of composite degradation, such as those caused by UV, thermal, or water immersion, also cause Young's modulus to decrease (Figures 8.14 and 8.15).[32,88] Thermal aging (Figure 8.14) causes a drop in Young's modulus at lower concentrations of filler followed by an increase. Similar effects were produced by other fillers, such as iron oxide and graphite.

Samples of epoxy resin filled with glass microspheres have a reduced elastic modulus after water immersion. The loss of elastic modulus is more pronounced as

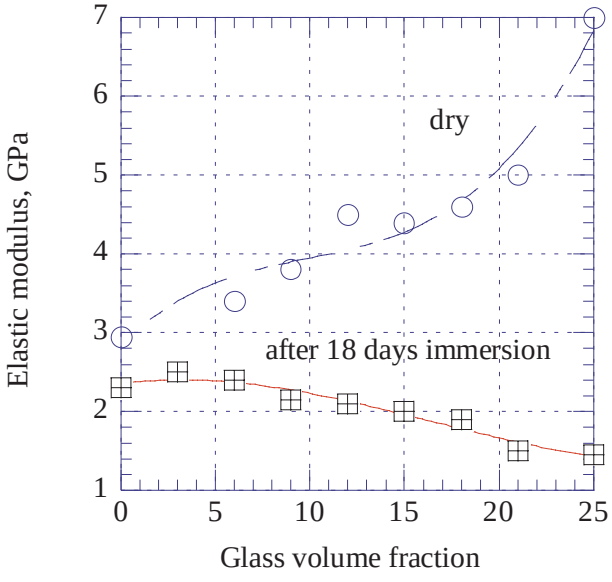

Figure 8.15. Young's modulus of epoxy reinforced with silane-coated glass microspheres vs. volume fraction of filler. [Adapted, by permission, from Lekatou A, Faidi S E, Lyon S B, Newman R C, *J. Mat. Res*., **11**, No.5, 1996, 1293-304.]

the concentration of microspheres is increased. But, without water immersion, the elastic modulus of the composite increases as the concentration of microspheres is increased (Figure 8.15).

8.4 FLEXURAL STRENGTH AND MODULUS

Flexural modulus is a convenient measure of composite stiffness. Fillers can contribute significantly to a stiffness increase.[3,6,20,23,24,27,28,31,33,41,42,50,64,70,71,74,92-101] The simple Einstein equation, Eq 8.2 permits a fit of experimental data as shown in Figure 8.16.[6] A different coefficient is needed for glass beads (a=-1.30) than for glass fiber (a=1.71). Flexural strength is about 1.5 to 2 times higher than tensile strength. The Einstein equation does not consider shape and particle size. It is known[50,94] that the flexural modulus depends on particle size. Larger particles of wood flour increase flexural modulus.[3]

The aspect ratio of the filler has significant impact on flexural modulus (Figure 8.17).[23] The values of coefficient, a, given on the graph are the values of coefficient from Einstein equation, Eq 8.2. This coefficient varies in proportion to aspect ratio of filler. The higher the aspect ratio the higher the steepness of graph.

Attempts to improve flexural strength by surface treatment of fillers have not, to date, been successful. A variety of silanes, titanates, and fatty acids and their derivatives have been used to coat magnesium hydroxide for use as a filler in polypropylene.[64] Almost all composites had inferior flexural properties. In the few cases where some improvement was seen, it was 10% more then the unfilled material.

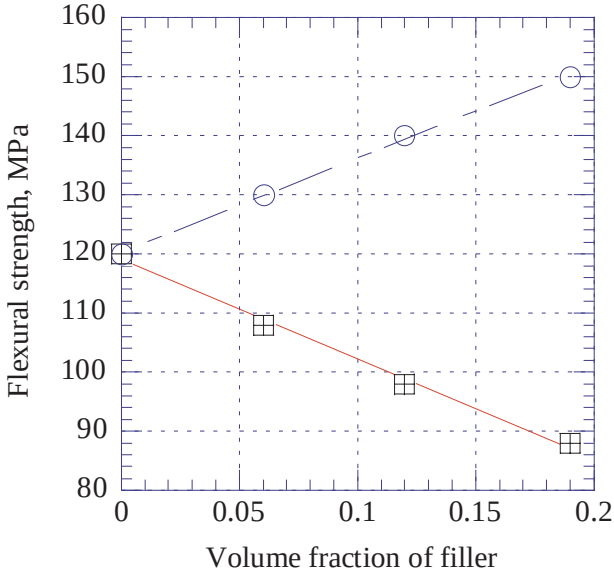

Figure 8.16. Flexural strength of POM vs. volume fraction of glass beads and glass fibers. [Adapted, by permission, from Hashemi S, Gilbride M T, Hodgkinson J, *J. Mat. Sci.*, **31**, No.19, 1996, 5017-25.]

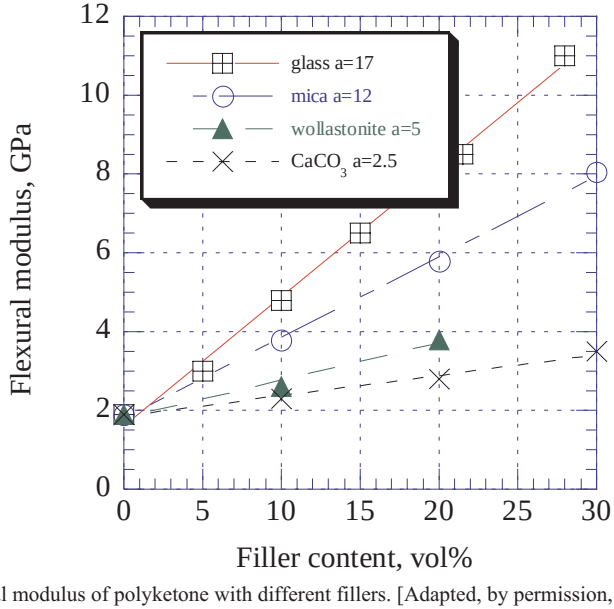

Figure 8.17. Flexural modulus of polyketone with different fillers. [Adapted, by permission, from Gingrich R P, Machado J M, Londa M, Proctor M G, Antec '95. Vol. II. Conference Proceedings, Boston, Ma., 7th-11th May 1995, 2345-50.]

Treatment of ultrafine talc with an acrylic modifier for use as a filler in rigid PVC always resulted in a gradual decrease of flexural modulus as the modifier concen-

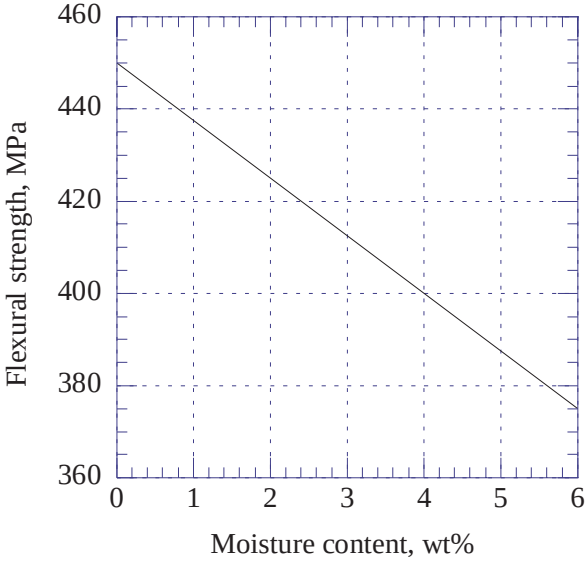

Figure 8.18. Flexural strength vs. moisture content in Kevlar reinforced epoxy. [Adapted, by permission, from Akay M, Mun S K A, Stanley A, *Composites Sci. Technol,* **57**, 1997, 565-71.]

tration was increased.[70] Similar results were obtained both with phosphate coated talc[33] and modified carbon black.[96]

Better mixing methods and processing techniques which align fibers in the composite seem to be the most promising avenues to improve flexural modulus with filler additions.[98-9] Mixing speed choice allows to increase flexural strength by 25%.

Finding a way to balance often conflicting requirements is the most challenging aspect of product development work. If a material is formulated to be fire resistant, UV stable, or moisture resistant, it may have inadequate mechanical properties. But with a careful and imaginative use of filler and filler coatings, a balance can be found.[92,100,101]

Figure 8.18 shows the effect of moisture content on the flexural strength of a composite.[92] The hygroscopic nature of both the fiber and the matrix contribute to the deterioration of the composite.

8.5 IMPACT RESISTANCE

Fillers improve the impact strength of the filled materials.[3-4,7,14,17,20,23-4,41,43-6,50,64,69-75,81,87,89,96,97,101-119] A model analysis of impact strength improvement is discussed below in the section on fracture and toughness.

The results of experimental studies which are summarized in Table 8.2 show the potential effect of different fillers on impact properties of filled materials. The information in Table 8.2 is presented in the same format as explained in introduction to Table 8.1.

Table 8.2. Effect of fillers on impact properties of filled materials

Filler/polymer	Conc. range, wt%	Impact strength increase (+) decrease (-), %	Refs.	Comments
PARTICULATE, INORGANIC FILLERS				
Calcium carbonate				
PEK	10−30	-55−-70	23	
PP	2	+45	112	improvement due to nucleation
PP	10−60	-40−+50	107	increase with stearate coating
PP	constant	0−+50	103	increases with particle % > 1 μm
PP	5−30 vol%	+20−+65	105	no adhesion; peak at 10 vol%
PP	5−30 vol%	+10−+25	105	perfect adhesion; peak at 10 vol%
PVC	2−45 vol%	+40−+150	104	peak value at 15 vol%
PVC	5−25	+20−+80	70	
Fly ash				
PP	5−20	-50−-65	87	
Glass beads				
PP	30 vol %	-35	89	
Kaolin				
PE	10−30	+140−+360	73	
Magnesium hydroxide				
PP	10−60	-27−-70	64	metal stearate coating can double IS
Mica, muscovite				
PA66	20−40	-30−-15	50	varies with particle size and amount
PBT	15−40	+15−-35	50	varies with particle size and amount
PEK	10−30	-50−-70	23	
PP	2−20 vol%	+5−+26	105	used in combination with $CaCO_3$
Mica, phlogopite				
PP	2−20 vol%	0−+15	105	used in combination with $CaCO_3$
Micaceous				
PP	10−60	0÷-20	43	hydrated K-Mg aluminosilicate
Talc				
PP/EP blend	1.2	+24	112	improvement due to nucleation
PP	10	-15	69	
PVC	5−20	+13−-15	71	
PVC	5−25	-13−-50	70	
Titanium dioxide				
PS	10−35	+9−+35	111	dispersion improves IS
Various				
PS	0.1	+15−+220	110	particle size determines IS
Wollastonite				
PA66	15−35	no change	13	
PEK	10−20	-35−-40	23	
FIBROUS FILLERS				
Carbon fiber				
PC	5−30	+40−+120	75	
Glass fiber				
PE	2−7	0−+7	7	
PEK	10−20	+10−+40	23	
PP	10−60	+300−+2750	102	constant fiber length at 6 mm
PP	25	+650−+1050	102	variable fiber length: 3−12 mm
PP	2−7	+100−+250	7	
Organic fillers				
Carbon black				
ABS	3	-20	114	varies depending on size and mixing
PP	15−60	no change	74	
PP copolymer	15−60	-30−+200	74	peak value at 30%

The data compiled in Table 8.2 show how impact strength can be improved. The following factors contribute to the improvement:

- Particle size (in many cases a certain range of particle size substantially increases impact strength)
- Particle shape (aspect ratio is the most important parameter; the use of fibers is the most certain method of impact strength improvement)
- Particle rigidity (hollow particles and fillers which have low hardness substantially decrease the impact strength)
- Interaction with the matrix (does not help in most cases; see for example calcium carbonate; in some cases (magnesium hydroxide) surface coating by metal stearate rapidly improves impact strength). Interaction with matrix is relevant in fiber reinforcements (see section on fracture resistance below)
- Concentration has a mixed influence (in fillers which improve impact strength, increased concentration increases impact strength)
- Nucleation (the presence of fillers or fillers with nucleating agents contribute to changes of crystallinity which increases impact strength)

Figure 8.19 shows the effect of the particle size of particulate fillers on impact resistance.[110] Several fillers were used in this study, including calcium phosphate, barium sulfate, calcium carbonate, and white carbon. The average particle diameters of these fillers ranged from 0.8 to 30 μm. The impact strength of composites containing different fillers is plotted against the average particle diameter. Particle size had a pronounced effect on impact strength whereas the influence of chemical composition was negligible. Maximum reinforcement was obtained with particles having diameter of 2 μm.

Figure 8.20 shows the effect of adhesion between the filler and the matrix on impact strength.[105] The maximum performance is obtained at low filler concentrations because interparticle distances and the formation of agglomerates are the controlling factors in impact strength improvement. If particles have perfect adhesion, the matrix is constrained to a greater degree because of matrix interaction with filler surface, leading to additional embrittlement of the material.

8.6 HARDNESS

Literature contains little data on the effect of fillers on hardness but what is available indicates that the addition of fillers increases hardness.[18,34,40,65,120-3]

Figure 8.21 explains that the reasons for this increase of hardness are more complicated than the increase caused by adding a harder material.[120] Fillers which have relatively large particle size do not interact and therefore their effect on hardness is due to their higher hardness. But the gain in hardness is very small because these particles are surrounded by an elastic matrix which moderates the effect of their hardness. Much larger gains are observed with semi-reinforcing grades due to the formation of an interlayer with mechanical properties more similar to the filler than to the matrix. In this case, the actual size of the particle is increased by the

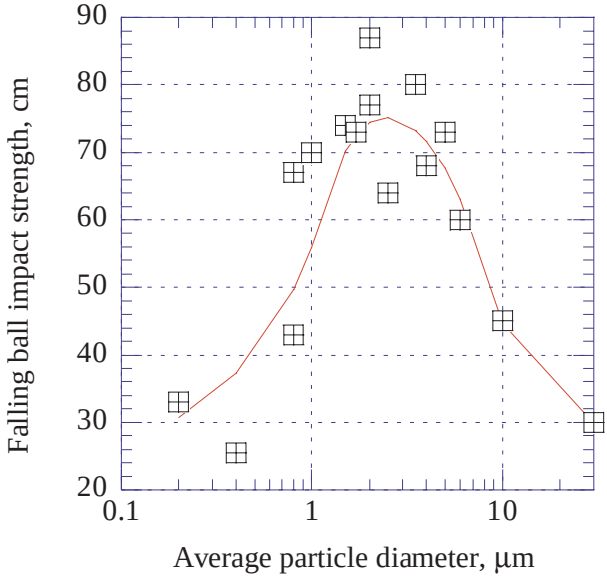

Figure 8.19. Falling ball impact strength vs. impact strength of filled polystyrene. [Adapted, by permission, from Mitsui S, Kihara H, Yoshimi S, Okamoto Y, *Polym. Engng. Sci*., **36**, No.17, 1996, 2241-6.]

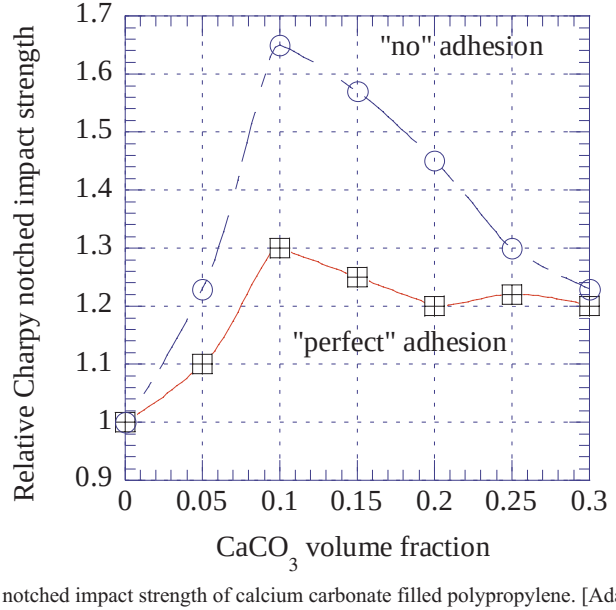

Figure 8.20. Charpy notched impact strength of calcium carbonate filled polypropylene. [Adapted, by permission, from Jancar J, Dibenedetto A T, Dianselmo A, *Polym. Engng. Sci*., **33**, No.9, 1993, 559-63.]

thickness of its adsorbed layer, therefore even small particles occupy a substantial space in composites. Reinforcing fillers introduce another variable related to formation of physical crosslinks which can be very numerous because of the small size

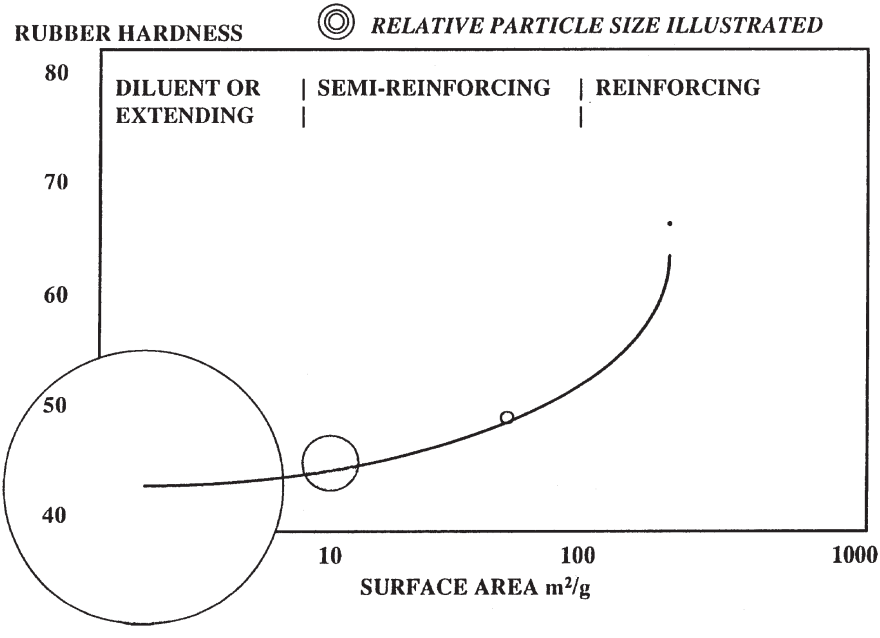

Figure 8.21. Rubber hardness vs. surface area of silica filler. [Adapted, by permission, from Evans L R, Meeting of the Rubber Division, ACS, Montreal, May 5-8, 1996, paper D.]

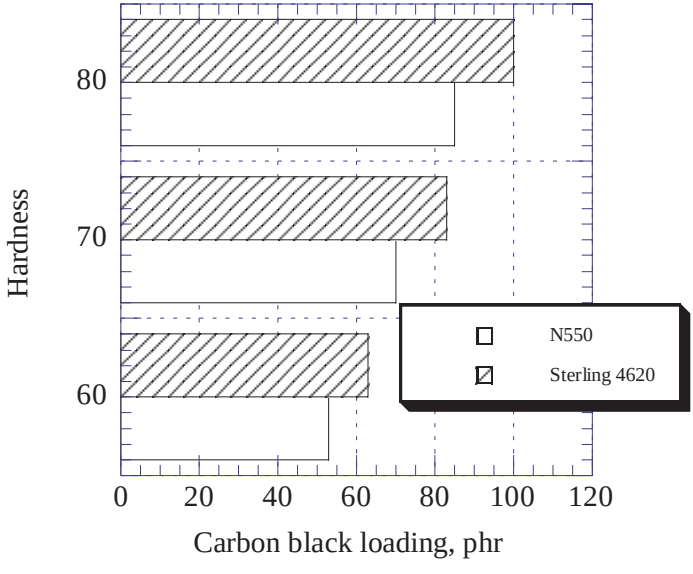

Figure 8.22. Carbon black loading for the same hardness. [Adapted, by permission, from Monthey S, Duddleston B, Podobnik J, *Rubb. World*, **210**, No.3, 1994, 17-9.]

of the particles. These physical crosslinks further reinforce the rubber resulting in its increased hardness.

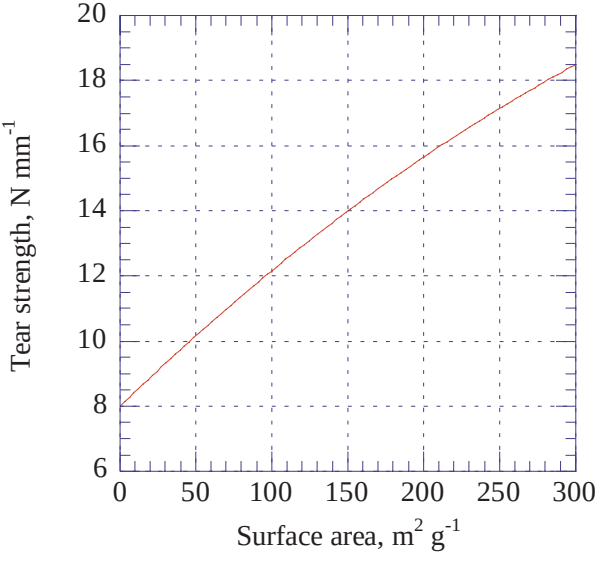

Figure 8.23. Silicone rubber tear strength vs. surface area of silica. [Data from Okel T A, Waddell W H, *Rubb. Chem. Technol*., **68**, No.1, 1995, 59-76.]

Figure 8.22 shows that the same hardness can be obtained by a wide range of levels of carbon black.[121] It is possible to add more carbon black and retain the same hardness. So, other properties such as compression set, can be improved without sacrificing the elasticity of the product.

Small additions of non-interacting fillers cause only small changes in product hardness. Usually, such additions produce a 10-20% increase in the hardness compared to unfilled material.[18,34,40,65,120,123]

8.7 TEAR STRENGTH

Tear strength data are very limited.[18,34,66,123-7] Tearing energy is given by the following equation:

$$G_c = 2kcW \qquad [8.12]$$

where:

k	function of extension ratio
c	crack length
W	strain energy density on the crack path

This equation indicates that tear strength can be increased by modulation of strain energy. A straight tear line with a smooth surface of tear path is indicative of low tear strength. Filler can improve tear strength in two ways. It may either form obstacles in the tear path which disrupts the smooth tear surface and changes the crack direction or by interacting with the matrix and adhering to it so that stress is transferred to the matrix over larger surface area.

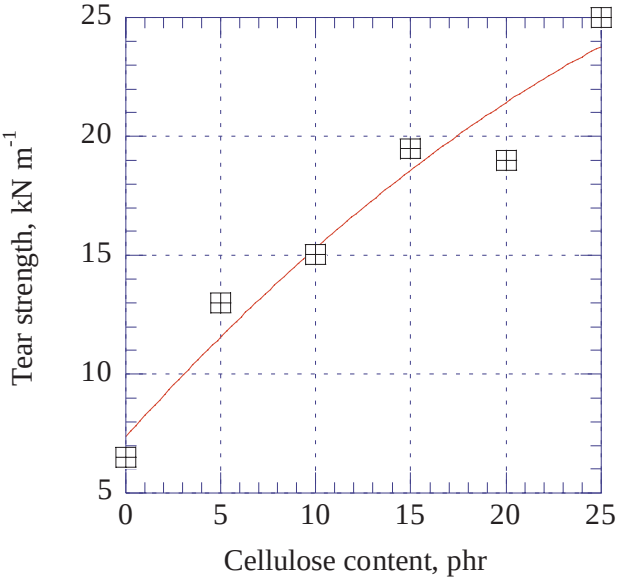

Figure 8.24. Tear strength of NR/BR vs. the amount of cellulose. [Data from Vieira A, Nunes R C R, Visconti L L Y, *Polym. Bull.*, **36**, No.6, 1996, 759-66.]

A filler with a high surface area increases the interaction with the matrix and thus increases tear strength (Figure 8.23).[125] When rubber is filled with silica the large surface area of the silica interacts with the rubber and adheres to it. This adhesive interaction allows energy to be stored or dissipated.

Fibers, due to their high aspect ratio, are the most efficient method of improving tear strength (Figure 8.24).[18] Even such weak fibers as cellulose fibers can increase tear strength by a factor of 6. Fibers form large obstacles in the path of crack growth. Fibers with better adhesion to matrix are more efficient.

The quantities of multifunctional additives used must be selected with care as each type and grade of carbon black requires a specific but different amount to achieve optimum performance. To achieve optimum adhesion, the concentration of additive should coat the surface of carbon black with a monomolecular layer. Building additional layers on the carbon black surface reduces adhesion which also reduces tear strength.

8.8 COMPRESSIVE STRENGTH

Compressive strength depends on the stiffness of the material, thus, all of the parameters which affect stiffness, including the effect of fillers, influence compressive strength.[17,79,92,95,128-9] The following equation associates compressive strength with other mechanical properties:

$$\sigma_{cc} = KG_R = K\left[\frac{E_\tau}{2(1+\nu)}\right] \qquad [8.13]$$

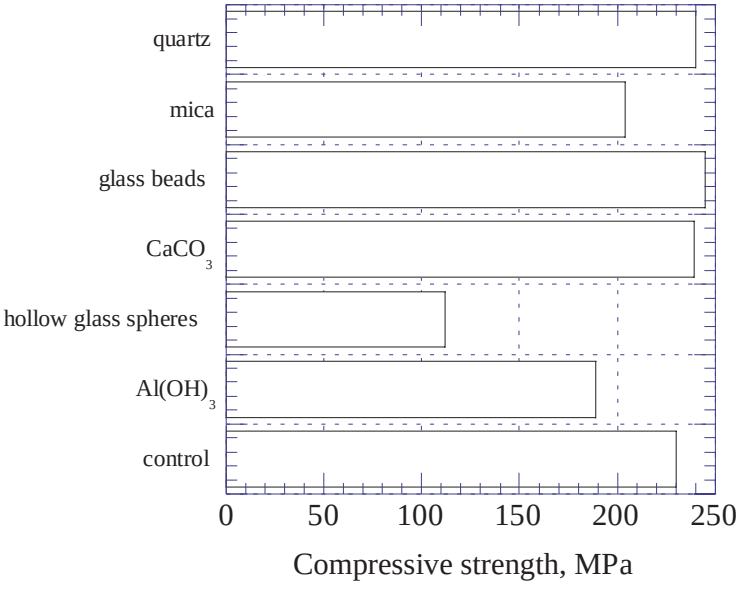

Figure 8.25. The effect of particulate fillers on the compressive strength of epoxy resin. [Adapted, by permission, from Yang Q, Pritchard G, *Polym. & Polym. Composites*, **2**, No.4, 1994, 233-9.]

where

σ_{cc}	compressive strength
K	constant
G_R	matrix shear modulus
E_τ	Young's modulus
ν	Poisson's ratio

This equation shows that the parameters which affect Young's modulus may affect the compressive strength. Figure 8.25 shows results for several fillers.[95] Aluminum trihydrate, hollow glass beads, and mica decrease compressive strength. The first two fillers are found to decrease Young's modulus as well. It is not clear why mica caused a decrease in compressive modulus. It would be expected to increase it. Remaining fillers increased compressive strength.

It was previously reported (Figure 8.18) that moisture reduces flexural strength of Kevlar filled epoxy. Figure 8.26 shows that moisture reduces its compressive strength.[92]

8.9 FRACTURE RESISTANCE

The fracture resistance of a material depends on all of the properties which have been discussed including tensile strength, yield stress, elastic modulus, flexural strength, and impact resistance, all of which depend, in part, on fillers. Fillers, consequently, are important determinants of fracture resistance.[4,6,10,26,32,56,73,87-8,104-5,109,116,125,130-45] Only those phenomena which are related

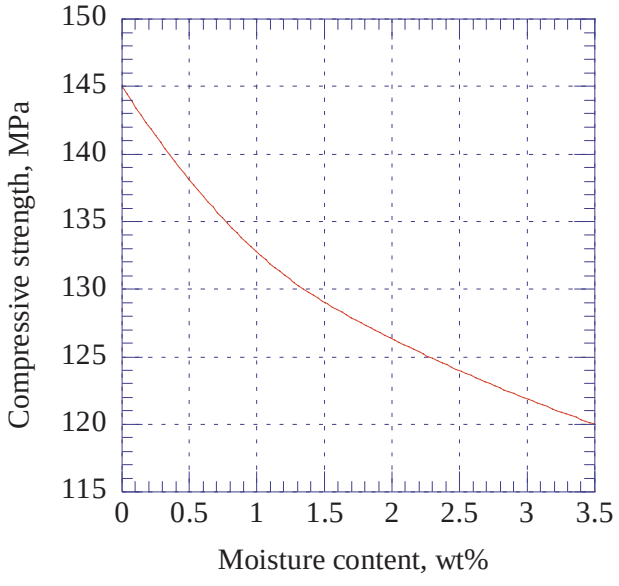

Figure 8.26. Compressive strength of Kevlar reinforced epoxy vs. moisture content. [Adapted, by permission, from Akay M, Mun S K A, Stanley A, *Composites Sci. Technol,* **57**, 1997, 565-71.]

to impact, flexural, or tensile stresses which can cause materials to fail. All phenomena related to cyclic forces are discussed under fatigue in a separate section.

This discussion includes the following:

- Modes of fracture
- Mechanism of fracture
- Microstructure of filler inclusions
- Changes in matrix due to impact
- Material toughening
- Methods of fracture prediction and modelling

Five fracture modes were observed during tensile experiments (Figure 8.27).[133] The most ductile compositions fracture during the strain-hardening (mode A) or the neck propagation (mode B). Modes C and D are typical of quasi-brittle fracture. A thinned region is formed at the neck formation (mode C). In this case, stress drops to the draw stress. In mode D, specimens fracture through macro-shearbanding. These bands are formed across the specimen and fracture occurs after a yield maximum is exceeded. Mode E is a brittle failure perpendicular to the loading direction. The fracture occurs before the yield point. The description of the mechanisms of these modes of fracture which follows is based on SEM observations of the fracture of calcium terephthalate and calcium carbonate filled thermoplastic polyester.[134]

The mechanism of fracture according to mode A is given by Figure 8.28.[134] The fracture surface had a rough region where a crack was propagated by a ductile

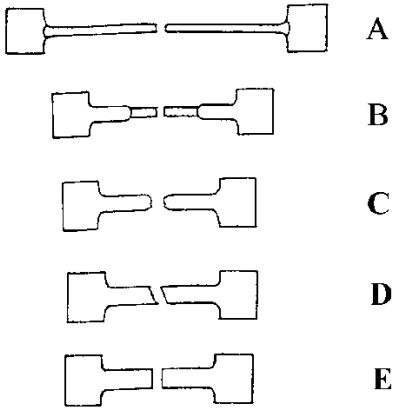

Figure 8.27. Schematic representation of the five tensile fracture modes. [Adapted, by permission, from Li J X, Silverstein M, Hiltner A, Baer E, *J. Appl. Polym. Sci.*, **52**, No.2, 1994, 255-67.]

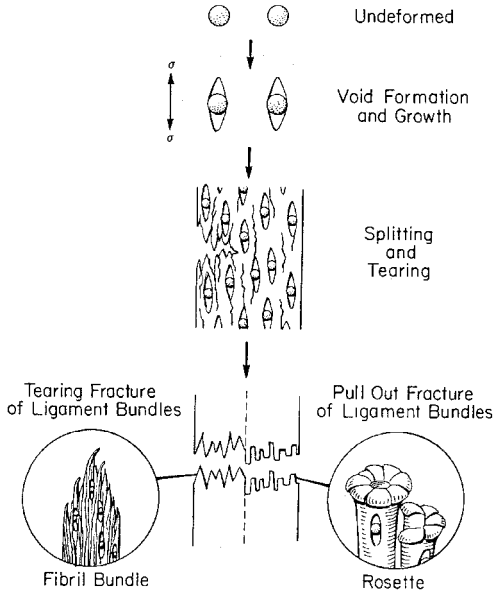

Figure 8.28. Schematic representation of mode A fracture. [Adapted, by permission, from Li J X, Hiltner A, Baer E, *J. Appl. Polym. Sci.*, **52**, No.2, 1994, 269-83.]

tearing. Strain hardening enables the polymer to sustain these loads. At a low concentration of filler (typical of mode A behavior), there is enough polymer matrix to withstand an external load without fracture. The surface has a pullout region (the initial fracture site) and a quasi-cleavage rosette region (where continuation of tearing occurs). The morphological features include debonded particles and elongated voids. Fracture occurs when the local strain in the ligaments reaches the fracture strain of the matrix. The formation of a rosette pattern requires a certain amount of polymer to be present and thus it will occur only at very low filler loadings.

Figure 8.29 shows the mechanism of fracture according to mode B.[134] Void formation and growth is similar to the previous mechanisms. The differences include the coalescence of voids and a singular tearing fracture initiated by a critical size of void created from coalescence. The fracture initiates from either the side or the center (mode A from the side only) and there is no rosette region. Fiber bundles are short and small in diameter.

Figure 8.30 shows the mechanism of fracture by mode C.[134] There was also a void formation and coalescence occurred in this specimen but only in lateral direction. Fracture was initiated from the center and had numerous secondary cracks. This mode of failure is typical of critical volume fraction of filler where the

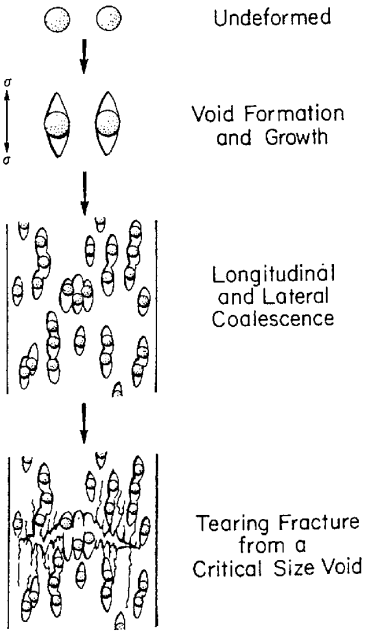

Figure 8.29. Schematic representation of mode B fracture. [Adapted, by permission, from Li J X, Hiltner A, Baer E, *J. Appl. Polym. Sci*., **52**, No.2, 1994, 269-83.]

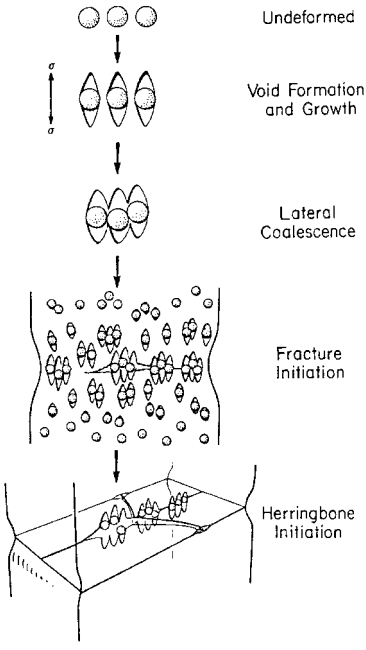

Figure 8.30. Schematic representation of mode C fracture. [Adapted, by permission, from Li J X, Hiltner A, Baer E, *J. Appl. Polym. Sci*., **52**, No.2, 1994, 269-83.]

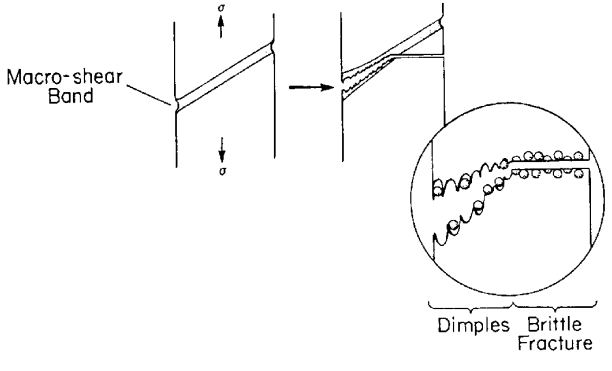

Figure 8.31. Schematic representation of mode D fracture. [Adapted, by permission, from Li J X, Hiltner A, Baer E, *J. Appl. Polym. Sci*., **52**, No.2, 1994, 269-83.]

particles are sufficiently close to diminish the sizes of the ligaments which are needed to resist fracture.

Figure 8.31 shows the mechanism of fracture by mode D.[134] Fracture was initiated at one side and propagated at an angle to the other side. As the rate of crack development increased, the fracture path deviated to become almost perpendicular to the direction of loading. This part did not exhibit the stress-whitening effect which indicates brittle fracture. Particles in this specimen were not debonded but some were cracked (see Figure 7.31). In fractures

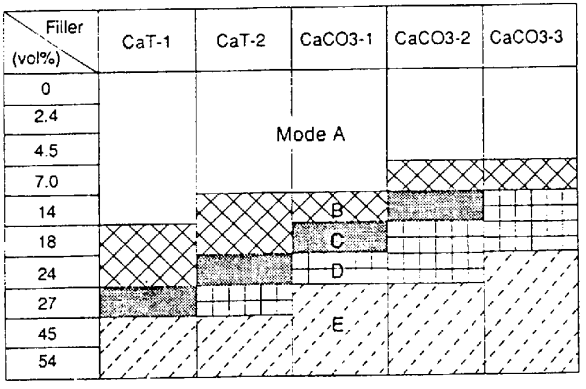

Figure 8.32. Map of fracture modes for various fillers and their concentrations. [Adapted, by permission, from Li J X, Silverstein M, Hiltner A, Baer E, *J. Appl. Polym. Sci.*, **52**, No.2, 1994, 255-67.]

by mode E, there was no indication of debonding but the particles themselves fractured along with the undeformed matrix.

Figure 8.32 shows the effect of filler type and concentration on the mode of fracture.[133] Several factors are responsible for the behavior. CaT (calcium terephthalate) fillers have good adhesion to the matrix and have an elongated shape. $CaCO_3$ (1) and (2) are both untreated fillers of smaller particle sizes (2.2 and 4.1 μm, respectively). $CaCO_3$ (3) is a stearate coated filler (better dispersion, but poor adhesion to matrix) with a particle size of 6.1 μm. The mode of fracture depends on filler concentration, the degree of adhesion to the matrix, and particle size.

While we have a comprehensive picture of tensile fracture modes, a similar picture of impact fractures is yet to be developed.[104] Composite behavior during impact is more complex than the behavior during tensile stress. Attempts at mathematical modelling are being made. The steps including crack initiation, propagation, yield, crazing, voiding and debonding (essentially similar to that discussed above) are being analyzed.

The way in which a filler is incorporated has an effect on fracture resistance. Figure 8.33 shows a schematic representation of the microstructure of fillers.[141] The rubber particles are generalized as rubber particles added in a toughening process (a), rubber or polymer coating in core-shell microstructure, bound polymer, or surface coating (b).

Figure 8.34 shows the results of impact on composites containing such particles.[141] Fillers without a coating allow the formation of numerous microcracks which weaken the material. Rubber particles lower the effect of impact and microcracking. Fillers coated by rubber (polymer) are more effective due to formation of yielding zone. This explanation also forms immediate question regarding the thickness of such a coating. A thick coating lowers toughness due to increased elastomeric behavior. A discussion of this and other structural phenomena follows.

Several characteristics of the matrix and filler-matrix interphase are involved in material toughening. These include: the particle size of filler, interfacial adhesion, filler concentration (already discussed), filler surface composition, the crystallization of the matrix, shell thickness, stress whitening, and strain hardening.

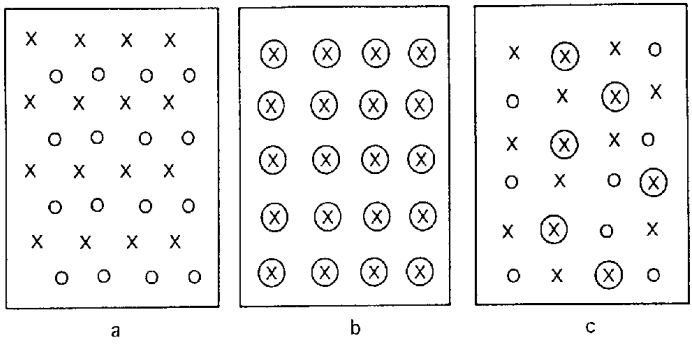

Figure 8.33. Schematic representation of three representations of microstructure of fillers (×) and rubber particles (❍) in polymer matrix. [Adapted, by permission, from Yu Long, Shanks R A, *J. Appl. Polym. Sci.*, **61**, No.11, 1996, 1877-85.]

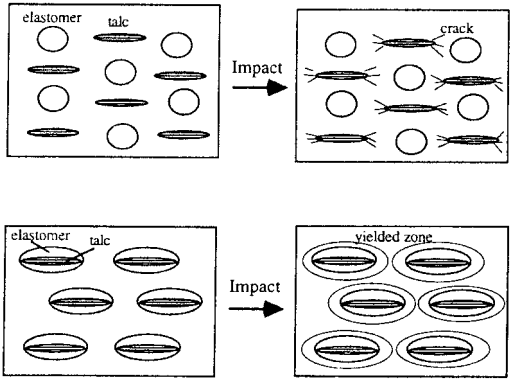

Figure 8.34. Morphological model of impact fracture of composites. [Adapted, by permission, from Li J X, Silverstein M, Hiltner A, Baer E, *J. Appl. Polym. Sci.*, **52**, No.2, 1994, 255-67.]

The effect of filler surface composition can be exemplified by a simple copper filler.[26] Two types of copper spheres were used in polyamide-11 composites. Both grades were produced by atomization but one filler had an oxidized surface whereas the other was reduced to pure copper. The mechanical properties of the copper composite were improved when oxidized particles were used because it had rougher surface which gave better adhesion. SEM micrographs showed that fracture surfaces were different in each case. The fracture path avoided the oxidized copper particles and failure occurred in the matrix whereas large debonded areas were seen on the reduced copper. This is an example of good mechanical adhesion being developed on a rough surface. The improved adhesion contributed to a change in fracture mode from adhesive to cohesive failure. Various methods used to enhance adhesion are discussed in Chapter 6. The organization of the interphase can also increase adhesion as discussed in Chapter 7. The thickness of shell (or interphase) is critical for materials toughness. To obtain a higher modulus than that of the matrix, a very thin shell is required along with very good adhesion. Increasing shell thickness rapidly lowers the rigidity of the material.

The addition of small particles of rubber to brittle polymers is the frequently used method to toughen materials. The improvement is due to increased crack growth resistance due to cavitation of rubber particles followed by deformation and crazing.[143] The role of such particles is to redirect the stress and distribute it onto a larger surface area. With that in mind, a theory was put forward that perhaps rubber particles are not necessary at all. The concept was tested by comparing the effect of rubber particles and holes created by the incorporation of thin wall latex particles. Figure 8.35 shows a fracture surface of epoxy modified with 10 vol% of such holes.[143] The particle sizes of latex particles were 0.4 and 1 μm and their walls were very thin. Control experiments were conducted with rubber particles having particles size of 0.2 and 0.55 μm. The fracture toughness of epoxy filled with holes was 2.30 and 1.95 MPa $m^{1/2}$ and of the rubber containing samples 2.05 and 2.2. The incorporation of particles may have affected crystallization, so DSC analyses were conducted which indicated no difference between filled and unfilled material. This example shows the importance of the matrix in the mechanism of toughening (since holes by themselves could not contribute to toughening).

Three phenomena are responsible for the response of a material to stress: the strain hardening, crazing, and stress whitening. The first two phenomena are completely beyond the scope of this book. Each increase mechanical performance of the matrix by orientation then crystallization of the matrix to counterbalance crack propagation. Stress whitening is a change of appearance around the stressed area which is thought to originate from void formation by separation of the polymer-filler interface. It is known from studies on silica in silicones that stress whitening can be decreased by reducing the pH of the silica and by lowering the Na_2O content.[125] Both factors improve surface wetting and improve adhesion.

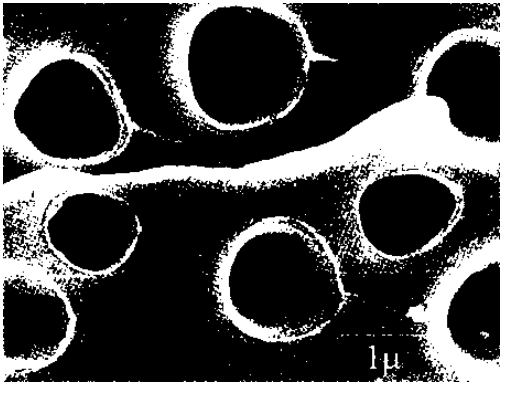

Figure 8.35. SEM micrograph of the fracture surface of an epoxy resin modified with 10 vol% latex particles. [Adapted, by permission, from Bagheri R, Pearson R A, *Polymer*, **36**, No.25, 1995, 4883-5.]

Many mathematical methods have been developed to interpret data. Some, more common models are given below. Fracture strength can be calculated from modified Einstein equation:

$$\sigma_c = \sigma_m(1 - 1.21\phi^{2/3}) \qquad [8.14]$$

where:

σ_c fracture strength of the composite

σ_m fracture strength of the matrix
ϕ filler volume fraction

This equation applies to systems in which there is no adhesion between the filler and the matrix. The equation predicts that the fracture strength of the composite is reduced as the filler concentration increases.

For random-packed monodisperse spheres where the concentration range is $0.56>\phi>0$, the following equation applies:

$$\sigma_c = \sigma_m(1+1.06\phi^2) \qquad [8.15]$$

This equation predicts that there will be some small gains in fracture strength as filler concentration increases. For fiber-filled composite the following equation was found to be supported by experimental data:[6]

$$\sigma_c = \sigma_m(1+1.64\phi) \qquad [8.16]$$

This equation explains why fiber reinforcement is so important in increasing fracture resistance. The above equations are important for basic classification of fillers in terms of their influence on fracture resistance but they are deficient in describing the effect of the matrix and the interaction with filler.

One method used is the energy rate interpretation of the J-integral. It is assumed that J has two constant values one at the crack initiation point, J_c, and the other at the failure point, J_R, given by equations:[109]

$$J_c = -\frac{1}{B}\frac{\Delta U_c}{\Delta a} \qquad J_R = -\frac{1}{B}\frac{\Delta U_T}{\Delta a} \qquad [8.17]$$

where:
B specimen thickness
U_c energy of initiation
a crack length
U_T total energy of fracture

The values of these two energies can be found by plotting U per unit thickness (U/B) vs. a. J-values can be determined from the slopes of the lines. Plotting J-values against the volume fraction of filler permits an estimate of the effect of filler on crack initiation and on the energy of fracture.

Other methods of data interpretation include the calculation of critical stress intensity (fracture toughness),[4] crack growth rate,[142] fracture energy,[104] and fracture resistance.[104] These models predict stress distribution, and rheological behavior of the matrix around the particle.

8.10 WEAR

The abrasive wear of plastics occurs as a result of strong adhesive interaction, fatigue, macroshearing, abrasive action, thermal and thermooxidative interaction, corrosion, cavitation, etc. Fillers are involved in these processes because mineral

fillers are abrasive and cause wear of the mating surfaces, other fillers are used to reduce wear.[146-50]

The wear volume of plastic material is given by equation:

$$W_s = K\frac{\mu P}{E}\frac{DW}{I_s} \qquad [8.18]$$

where:

K	proportionality constant
μ	coefficient of friction
P	force
E	modulus
D	sliding distance
W	load
I_s	interlaminar shear strength

A filler used as a wear decreasing additive should not lower the permissible strain, μP/E.

Both the matrix and the filler contribute to wear resistance. Typical polymers used in these applications include polyamide, polyacetal, polybutene terephthalate, and polycarbonate.[150] These polymers have the right balance of required properties, such as low friction coefficient, good mechanical properties, impact strength, and dimensional stability. Filler selection depends on the value of its friction coefficient, its having a minimal influence on the mechanical properties of the matrix polymer, and its good adhesion to the matrix. Frequently, it is difficult to meet these criteria because fillers which have a low friction coefficient do not combine well with other materials. Polytetrafluoroethylene, frequently used as anti-wear additive, is such an example. The addition of 20% PTFE to polyamide-66 reduces its tensile strength by 40%. In order to compensate for this effect, PTFE is frequently used in combination with glass fibers. Glass fibers increase the abrasiveness of the material but also reinforce it and thus balance the losses due to the use of PTFE.

Typical fillers used for reduction of wear include PTFE, silicone, graphite powder, molybdenum disulfide, and aramid fibers. Good results were also reported with mica and zirconia combination.[151] Figure 8.36 shows the effect of mica and mica in combination with zirconia on the wear resistance of an epoxy resin.[151]

Figure 8.37 shows that additions of graphite and MoS_2 are capable of making PTFE even more wear resistant.[146] This effect is limited to a relatively small range of filler concentration because PTFE does not interact with fillers and its mechanical properties deteriorate rapidly as filler concentration increases. The addition of 40% filler (graphite or MoS_2) reduces the elongation from 240% to close to zero. Addition of only 20% filler reduces the elongation to about half of the unfilled value.[146]

Figure 7.9 illustrates the effect of fiber orientation on wear rate.[153-4] The surface roughness of the mating surfaces influences wear. Adhesion of fibers to the matrix and their dispersion are other essential parameters of the aramid fibers performance.[150] Large surface area of the aramid fibers caused mechanical inter-

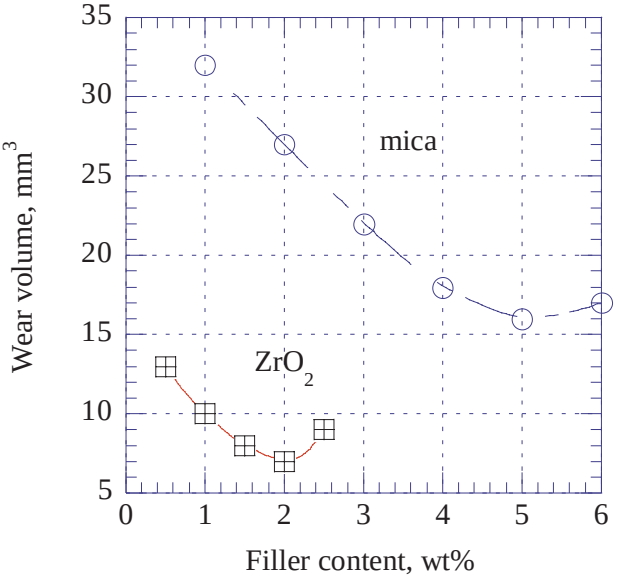

Figure 8.36. Wear volume vs. amount of filler. [Data from Srivastava V K, Pathak J P, *Polym. & Polym. Composites*, **3**, No.6, 1995, 411-4.]

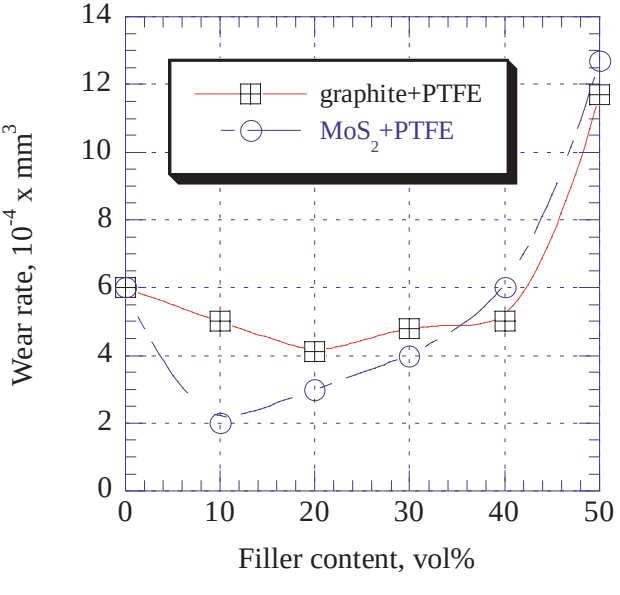

Figure 8.37. Wear rate vs. filler content. [Adapted, by permission, from Fengyuan Yan, Qunji Xue, Shengrong Yang, *J. Appl. Polym. Sci*., **61**, No.7, 1996, 1223-9.]

locking and limited their dispersion in the matrix. An application of a sizing agent increased adhesion but also caused the fiber to form bundles which were difficult to separate after cutting process. A special process oil was used to prevent bundling.

8.11 FRICTION

Table 8.3. Friction coefficient of some plastics

Polymer	Filler	Amount, wt%	Dynamic coefficient of friction
Polycarbonate	PTFE	10	0.12
Polycarbonate	Aramid	15	0.15
Polycarbonate	PTFE	15 15	0.10
Polyoxymethylene	PTFE Aramid Silicone	10 5 3	0.05
Polybutyleneterephthalate	PTFE	15	0.20
Polyethyleneterephthalate	PTFE	10	0.15
Polyamide-6	PTFE	15	0.23
Polyamide-6	PTFE Silicone	18 2	0.11
Polyamide-6,6	PTFE Glass fiber	15 30	0.26
Polyamide-6,6	PTFE Glass fiber Silicone	13 30 2	0.14
Polyamide-6,6	PTFE Carbon fiber	15 30	0.11
Polyamide-11	PTFE	15	0.31
Polyamide-12	PTFE	20	0.20
Polyamide, amorphous	PTFE	20	0.22
Polypropylene	PTFE Glass fiber	15 20	0.09
Polyurethane, thermoplastic	PTFE	15	0.32

This section adds information on the influence of filler on the wear behavior of plastics.[149,152-4] The friction coefficient of a material depends on the applied load according to the following equation:

$$\mu = KW^{0.3-0.4} \qquad [8.19]$$

where:
K proportionality coefficient
W load

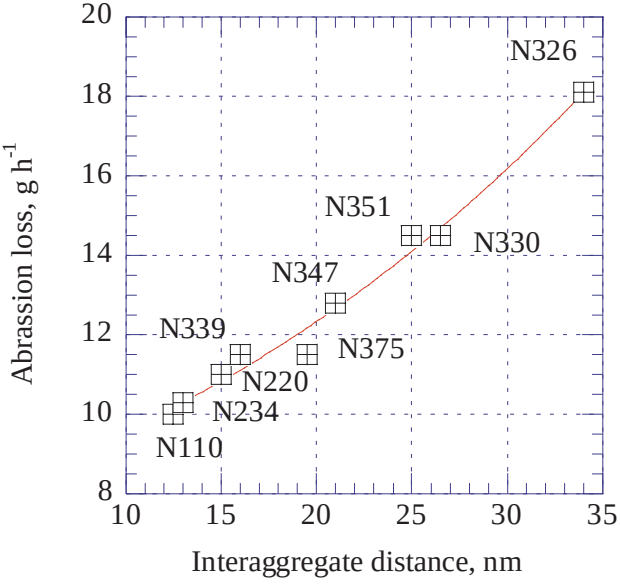

Figure 8.38. Abrasion loss of SBR containing different types of carbon black vs. interaggregate distance. [Adapted, by permission, from Patel A C, *Kaut. u. Gummi Kunst*., **47**, No.8, 1994, 556-70.]

Table 8.3 gives friction coefficients of plastics containing fillers intended as wear reduction additives.

Generally, the friction coefficient decreases as the load of filler increases but there is a critical quantity above which the friction coefficient decreases. The correct amount of anti-wear additive for a particular material and a particular applied load can be determined by simple morphological observation of the surface. The expected wear pattern forms surface debris whereas if the part is not wearing well its surface will melt and become shiny.

8.12 ABRASION

Two aspects of abrasion will be discussed, namely the abrasion resistance of filled materials and the use of fillers in the friction materials.[34,123,126,156-7] Each has its own specificity and differs from other two.

Rubber, due to its elastomeric properties, usually, has a low abrasion resistance. Fillers such as carbon black and silica can be added to impart abrasion resistance. Figure 8.38 shows the extent to which different grades of carbon black are abraded.[156] As interaggregate distance decreases the abrasion loss decreases as well.

Figure 8.39 shows that increasing the filler concentration decreases abrasion loss. Because of chemical interaction between the hydroxyl groups on clay and the ionic crosslinker in EPDM, clay reduces the abrasion loss more effectively than carbon black. Carbon black forms a weak interaction with the backbone

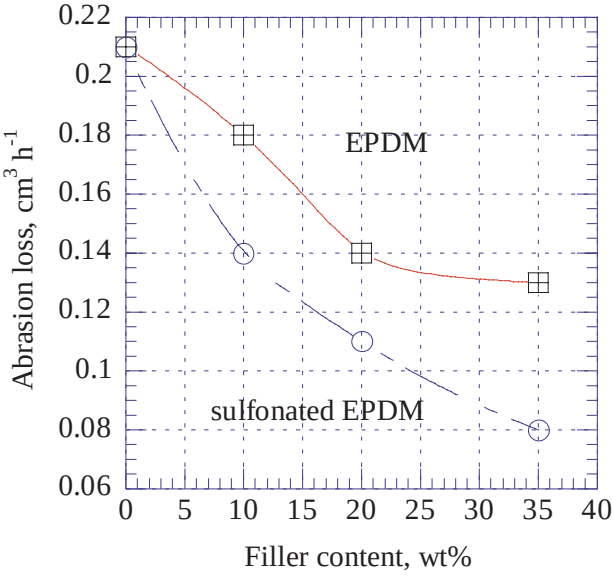

Figure 8.39. Abrasion loss of EPDM vs. filler content. [Data from Kurian T, De P P, Khastgir D, Tripathy D K, De S K, Peiffer D G, *Polymer*, **36**, No.20, 1995, 3875-84.]

chains.[34,123] Increased adhesion between the filler and the matrix contributes to an increase in abrasion resistance.[126] Studies on natural rubber filled with silica demonstrated this performance improvement. The adhesion between the filler and the matrix was increased by a multifunctional additive. As the concentration of the additive was increased the abrasion loss decreased.

Typical friction materials used in the automotive industry are brake pads and clutches.[157] In the past, asbestos was the filler of choice but after 1983, the use of asbestos was gradually phased out and alternative replacements were found after extensive tests on over 1200 different materials. There are three main technologies used for brake pad production: metallic brake linings, carbon-carbon composites, and resin-bonded friction materials. Resin bonded friction materials will be discussed here. The friction material must fulfill several requirements which makes the choice of filler a complicated process. In addition to a sufficient friction coefficient (typically 0.4-0.5), brakes should not suffer a substantial and long-lasting loss of friction during repeated cycles of overheating and returning to normal temperature. Brakes should recover quickly from friction loss due to exposure to water, they should have high tolerance to different magnitudes of load and wear. Meeting all these requirements is challenging. Fillers are seldom used alone but rather in combination. These may include a conductor to facilitate heat dissipation (metal powder, most frequently copper or brass), a particulate filler for surface filling and cost reduction (typical candidates are barytes, calcium carbonate, and clays) and reinforcement (fibers which can withstand heat and maintain mechanical and fric-

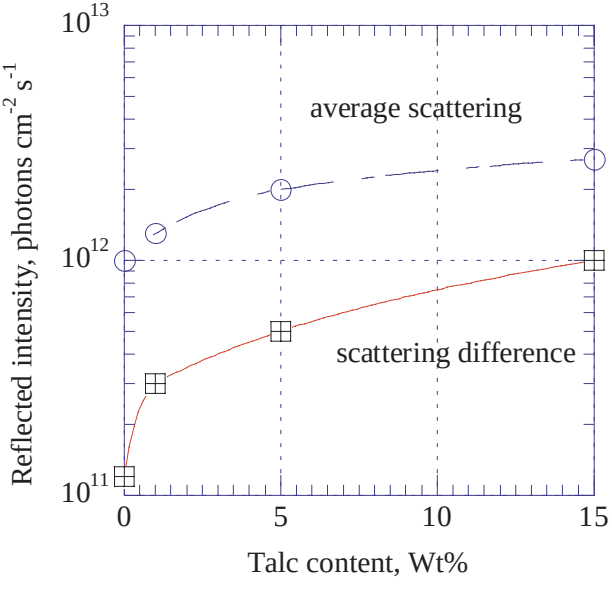

Figure 8.40. Average scattering and scattering difference vs. talc load in polypropylene. [Adapted, by permission, from Kody R S, Martin D C, *Polym. Engng. Sci*., 36, No.2, 1996, 298-304.]

tional properties, such as aramid, glass, carbon, steel, cellulosic). All fibers used today are still no match for asbestos which had thermal stability, high mechanical properties, and sufficient elasticity to prevent fracture (typical of glass and carbon fibers). The biggest challenge of new technologies is to overcome existing relationship between coefficient of friction and wear rate which makes more durable brakes less efficient.

8.13 SCRATCH RESISTANCE

In spite of the fact that scratch resistance is very important requirement only a limited number of credible studies have been done. This research is very difficult to conduct.[158-9] Recently, image analysis was employed to overcome some of the technical difficulties associated with the interpretation of observations. In addition to the damage of the scratch itself, the surrounding areas show stress whitening which adds to the perceived damage. The use of plastics in the automotive industry, especially the wide use of polypropylene makes these studies very important in the development of high quality finished products.

The method adapted in instrumental studies includes several steps: surface scratching using a controlled testing apparatus, analyzing the scratch area by reflected polarized light in an optical microscope, image acquisition, and analysis of the digital image.[158] Figure 8.40 shows of the data obtained when the scratch surface of talc filled propylene was analyzed. As the amount of talc was increased, scratch resistance decreased. The average scattering of reflected polarized light

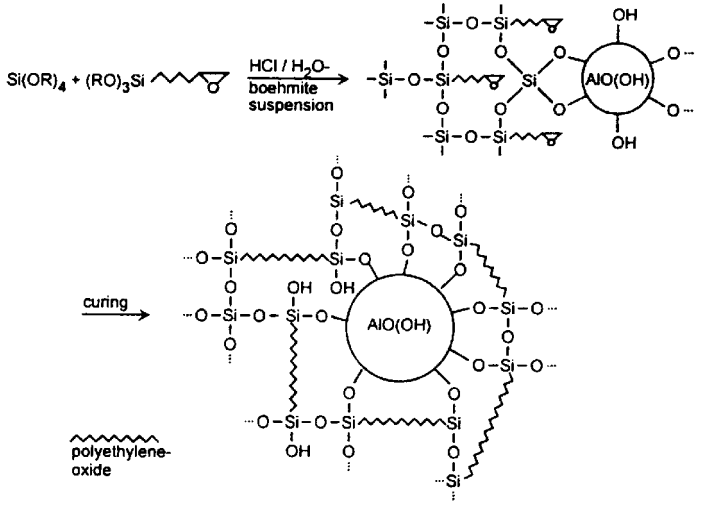

Figure 8.41. Reaction scheme and structural model of boehmite-based nanocomposite. [Adapted, by permission, from Schmidt H K, *Macromol. Symp*., **101**, 1996, 333-42.]

correlates with void formation due to the impact-related separation of filler from the matrix. The scattering difference is related to changes in chain orientation resulting from scratch damage. Results can be improved by increasing the adhesion between filler and matrix only an incremental improvement is possible because of an inherent deficiency in talc (low hardness).

Figure 8.41 shows the structure of a novel nanocomposite and how it was formed.[159] This nanocomposite has high scratch resistance. It is currently used for an optical lens coating. Its scratch resistance was increased by factor of 3 in the diamond scratch test when compared with conventional hard coatings and by factor of 2 in lens testing where lenses are rotated in drum of abrasive material. These excellent properties are due to a structure which makes both the filler and the matrix a singular, ordered material.

8.14 FATIGUE

Fillers contribute to the elastomeric properties of materials and thus affect the fatigue resistance of compounded products.[73,124,132,140,144,160-177] The discussion below includes:

- The principles governing fatigue resistance
- The mechanisms of fatigue deterioration of filled systems
- The effect of fillers on improvement of fatigue resistance

Paris' law relates crack propagation rate to stress intensity:

$$\frac{da}{dN} = C(\Delta K)^m \qquad [8.20]$$

where:

a	crack length
N	number of cycles
C, m	material dependent constants
ΔK	$= K_{max} - K_{min}$, stress intensity factor range

The values of constants C and m are not associated with any particular physical meaning. ΔK increases when filler load increases. This indicates that the filler increases fatigue resistance. Crack growth data can be conveniently obtained by interfacing tensile testing machine operating in a cyclic mode with a software/hardware combination capable of determining crack length at one cycle intervals.[140] The following equation is used to calculate results:

$$\left(\frac{da}{dN}\right)_n = \frac{a_{n+1} - a_{n-1}}{N_{n+1} - N_{n-1}} \qquad [8.21]$$

where:

n	iteration number

Figure 8.42 shows one outcome of such studies.[140] The addition of surface treated glass beads requires substantially higher stress to support the same growth rate of cracks compared with neat epoxy. Good adhesion and stress distribution are responsible for improvement.

The other factor which is important in fatigue resistance studies is related to dissipation of energy. The energy accumulated in the material due to extension must be dissipated. Energy dissipation is given by the equation:

$$W_d = \int_0^{2\pi} \sigma(t)\frac{d\gamma}{dt}dt = \pi G''\gamma_0^2 \qquad [8.22]$$

where:

W_d	energy dissipated in a complete strain cycle per unit volume
σ	stress response
γ	input strain
t	time
G′	loss modulus (G″ = G′tanδ)

Figure 8.43 shows difference in behavior between filled and unfilled materials.[174] There is a large difference in the energy stored by the two systems due to the reinforcing action of carbon black. Also, filled systems differ in their reaction to continuous stress. In a filled system, nonlinear behavior is observed due in part to the level of energy involved in cycling. This affects efficiency of energy dissipation and formed crosslinks.

Stress softening is a phenomenon related to filler reinforcement. When a material is extended to a certain strain, returned to zero strain and stretched again, the second stress-strain curve lies below the first one. There are several reasons for this phenomenon, including incomplete elastic recovery, conversion of the hard phase

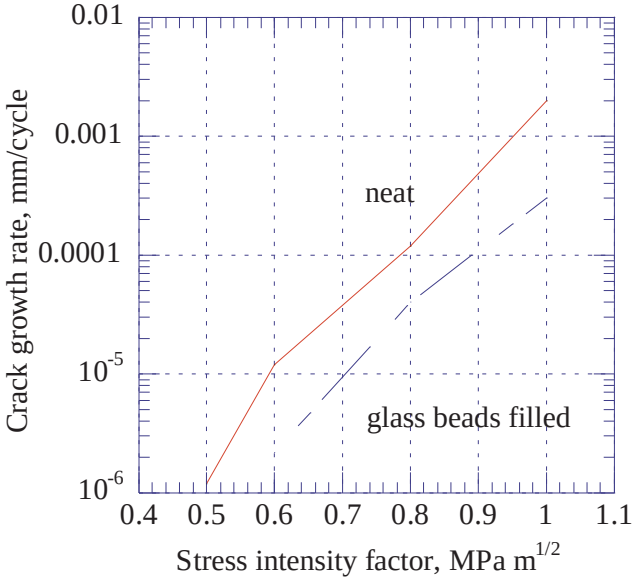

Figure 8.42. Crack growth rate of epoxy with and without glass beads vs. stress intensity factor. [Adapted, by permission, from Azimi H R, Pearson R A, Hertzberg R W, *J. Appl. Polym. Sci*., **58**, No.2, 1995, 449-63.]

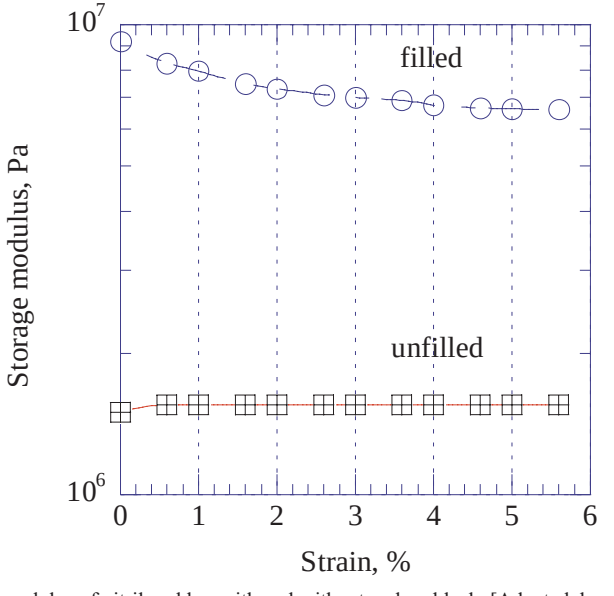

Figure 8.43. Storage modulus of nitrile rubber with and without carbon black. [Adapted, by permission, from Gownder M, Letton A, Hogan H, Antec '95. Vol. II. Conference Proceedings, Boston, Ma., 7th-11th May 1995, 1983-6.]

to soft phase, breaks in the network, and chain slippage from detachment points.[160]

The equation for loss of deformation energy gives a mathematical interpretation of this phenomenon:

$$\Delta W = \left[1 - \int_0^{\varepsilon} \sigma d\varepsilon \Big/ \int_0^{\varepsilon} \sigma_0 d\varepsilon\right] 100 \qquad [8.23]$$

where:

ΔW	loss of deformation energy
σ	stress value of second cycle (deformation)
ε	maximal strain
σ_0	stress value of the first cycle

The Mooney-Rivlin equation is frequently used to interpret experimental results related to stress softening:

$$g(\varepsilon) = 1 + \frac{C_2}{C_1}\frac{1}{\lambda} \qquad [8.24]$$

where:

$g(\varepsilon)$	damping function (based on the fact that the material's response does not remain proportional to the deformation)
C_1	elastic constant (a measure of the connectivity of network strands)
C_2	stress relaxation constant (contribution of trapped entanglements to the equilibrium modulus)
λ	extension ratio

Failure occurs in two steps: crack initiation and crack propagation. The examples above and some examples presented below show that the addition of filler may help in interfering with the propagation step. But the filler introduces inhomogeneity to the matrix and thus may contribute to crack initiation. In this respect the properties of the matrix are very important. If the matrix has a brittle character, its fatigue resistance depends on crack initiation. Once a crack is initiated, its propagation is a very fast process. In ductile matrix there is a larger resistance to crack propagation, therefore the introduction of a crack initiation site (e.g., fillers) is not as detrimental to overall fatigue resistance. Matrix-filler adhesion and the matrix character determine the influence of the filler on crack initiation.

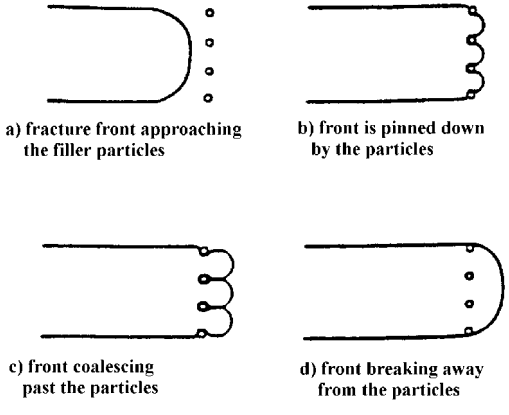

Figure 8.44. Crack front propagation slowed down by a pinning mechanism. [Adapted, by permission, from Azimi H R, Pearson R A, Hertzberg R W, *J. Appl. Polym. Sci*., **58**, No.2, 1995, 449-63.]

Crack propagation is affected by the properties of the filler and its interaction with

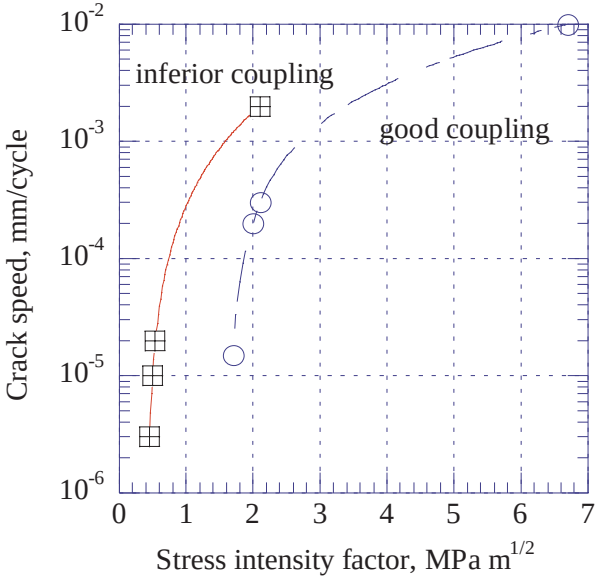

Figure 8.45. Effect of coupling on crack rate development in kaolin-filled HDPE. [Adapted, by permission, from Savadori A, Scapin M, Walter R, *Macromol. Symp*., **108**, 1996, 183-202.]

the matrix. Figure 8.44 shows the mechanism by which filler particles may slow crack propagation.[140] A crack front approaches filler particles which have good adhesion to the matrix. The front of the crack is slowed by filler particles because of their interaction with the tip stress field. Cavitation and coalescence of voids is followed by the matrix breaking away from particles and the crack front progressing to the next obstacle.[140]

Figure 8.45 shows experimental data from a different source[73] which confirms the pinning mechanism. Much higher stress intensity (ΔK from Eq 8.20) is required to support the same crack growth rate in material with good adhesion as compared with material with poor adhesion.

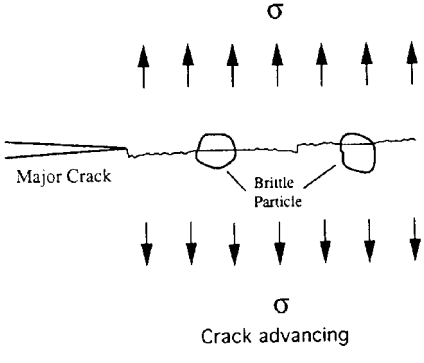

Figure 8.46. Crack growth mechanism. [Adapted, by permission, from Xu X X, Crocrombe A D, Smith P A, *Int. J. Fatigue*, **16**, No.7, 1994, 469-77.]

Figure 8.46 shows the effect of crack advancement on integrity of filler particle.[164] The advancing crack can be delayed by the pinning mechanism if stress is lower than adhesion and filler particle cohesion. If stress is higher than particle cohesion then particles may break. The

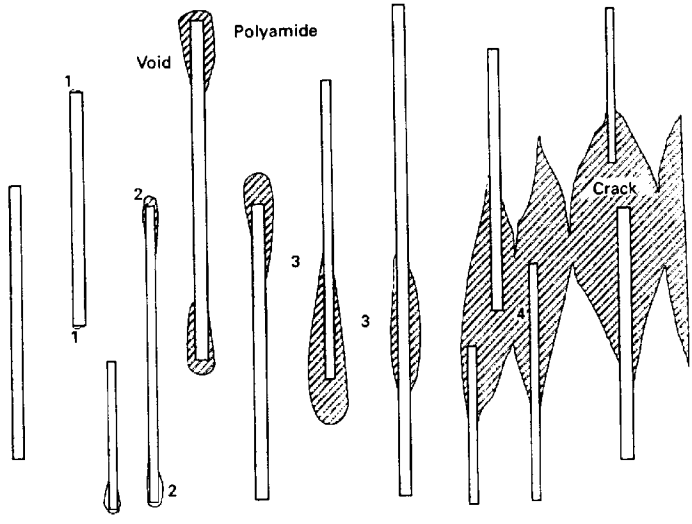

Figure 8.47. Failure mechanism in fiber reinforced system. [Adapted, by permission from Horst J J, Spoormaker J L, *J. Mater. Sci*., **32**, 1997, 3641-51.]

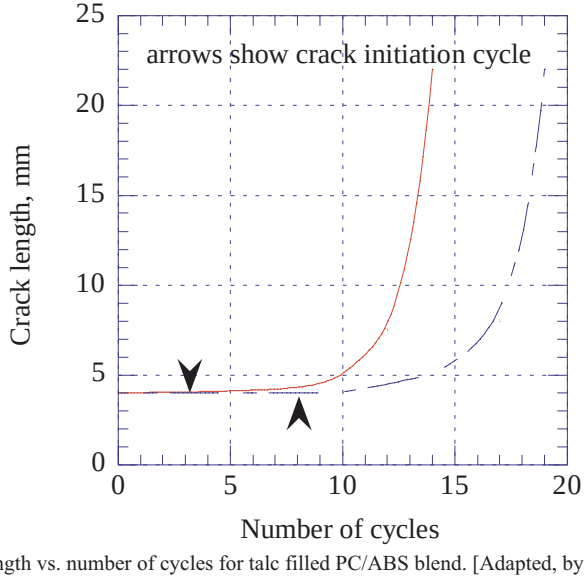

Figure 8.48. Crack length vs. number of cycles for talc filled PC/ABS blend. [Adapted, by permission, from Seibel S R, Moet A, Bank D H, Sehanobish K, Antec 95. Volume III. Conference proceedings, Boston, Ma., 7th-11th May 1995, 3966-70.]

experimental evidence of the operation of this mechanism is given in Figure 7.31.

The fiber debonding mechanism is given in Figure 8.47.[162] Several stages are involved, including debonding, void formation, coalescence, and finally crack formation. Because of a higher stress around the fiber ends, debonding is more likely

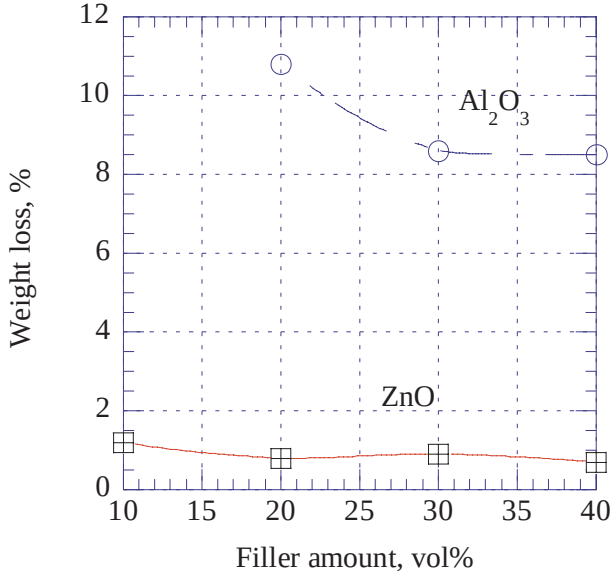

Figure 8.49. Weight loss vs. filler amount in PDMS. [Data from Visser S A, *J. Appl. Polym. Sci*., **64**, 1997, 1499-1509.]

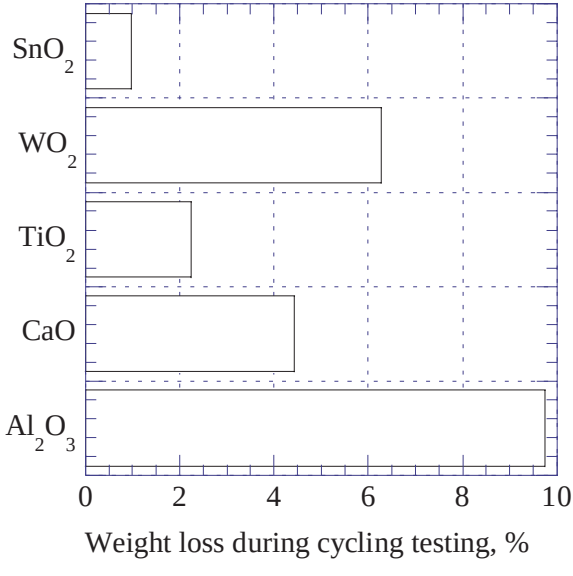

Figure 8.50. Weight loss vs. filler type. [Data from Visser S A, *J. Appl. Polym. Sci*., **63**, 1997, 1805-20.]

to occur in these areas. There is substantial evidence from SEM studies which confirms that such mechanisms operate in composites.

Several examples below illustrate the effect of fillers on fatigue resistance. Figure 8.48 shows that crack length depends on the number of cycles.[144,166] Talc in-

creases the time to failure by about 50%. Both crack initiation and crack propagation were improved by the addition of talc.

Figure 8.49 shows the effect of filler concentration on fatigue resistance.[170] The weight loss during the cycling stress experiment is caused by the reaction of ionic fragments with polymer chains. As a result of these reactions, volatile species are lost. In this experiment each sample was subjected to 60 cycles.

Figure 8.50 shows the results of similar studies for different fillers in PDMS.[169] In most cases the increased Young modulus of filled composite corresponds to less weight loss. This points again to the effect of interaction on failure resistance.

8.15 FAILURE

These remarks evaluate the effect of filler-related phenomena on failure of plastic materials.[80,90,175-182] Several reasons for the failure of plastics are filler related. They include delamination of laminated composite materials, debonding in particulate filled materials, stress cracking of filler particles, yielding, cavitation, and corrosion.

Failure analysis of composite pipe[182] shows that the majority of problems are related to bundling of fibers which prevents the binder from wetting the individual fibers, the porosity of the resin which allows penetration of the composite by corroding liquids, and a lack of adhesion between the matrix and a sand filler. All these failures can be substantially reduced and the useful life of pipes extended by application of proper technological practices. A high porosity in the binder layer increased corrosion rate which, in turn, reduced the original fiber strength to 1/3 of its initial value over a period of 10 years. With good fiber protection, mechanical strength was reduced by only 30%.[182]

Figures 8.51 and 8.52 show differences between the behavior of polypropylene filled with glass beads at different temperatures.[175] In both cases, the debonding between filler and the matrix requires the lowest level of energy and confirms that this is the most likely mode of failure. The volume fraction of filler has little effect on debonding, cavitation, and yielding at 0°C. At -60°C, yielding is improved by increasing concentration of filler. Debonding is initiated at the poles and begins plastic yielding in the matrix which ultimately leads to failure.[90] Strain required to initiate failure is reduced when the filler concentration is increased.[90]

The adhesion between the matrix and the filler has an important influence on the mechanism of failure. In polyester filled with quartz, uncoupled (low adhesion) quartz was delaminated from the matrix if the quartz particles were in the path of the crack growth. Silane coupled quartz particles showed many instances of particle cracking on the pathway of crack growth. Apparently, adhesive forces were higher than the cohesion of filler material.[178]

In polymer blends, the distribution of filler between the two or more component polymers of blends influenced tensile, tear, and fatigue failures. For example,

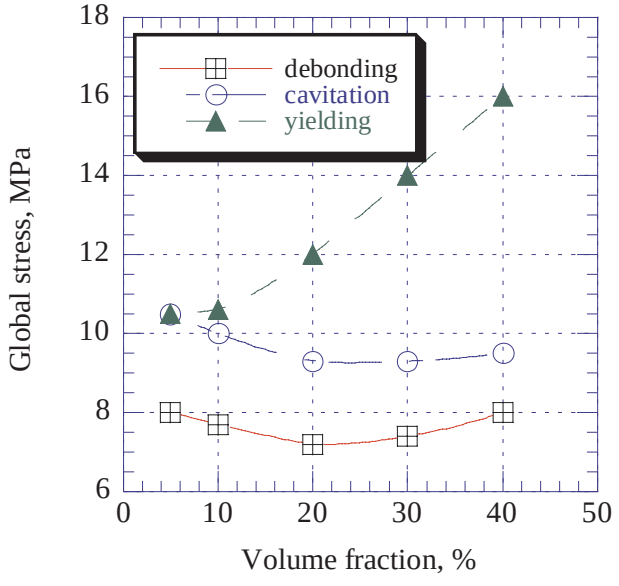

Figure 8.51. Global stress vs. volume fraction of glass beads in polypropylene at -60°C. [Adapted, by permission, from Asp L E, Sjogren B A, Berglund L A, *Polym. Composites*, **18**, No.1, 1997, 9-15.]

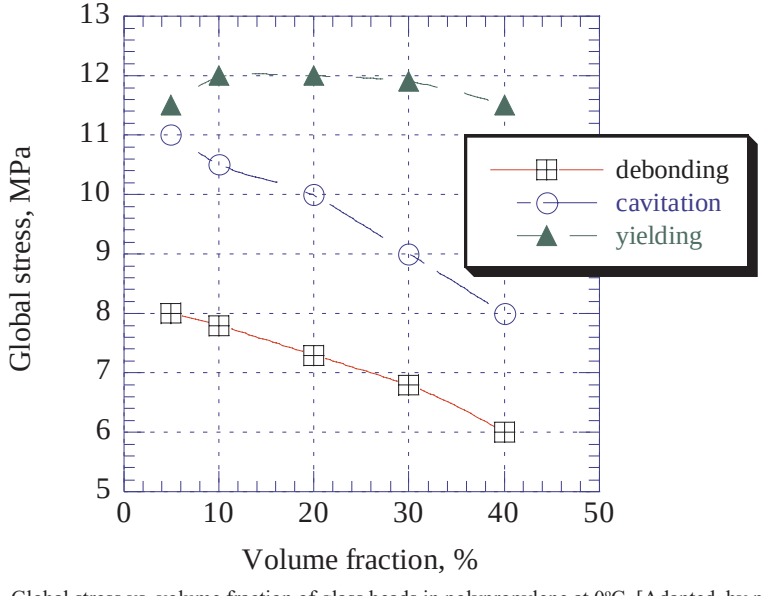

Figure 8.52. Global stress vs. volume fraction of glass beads in polypropylene at 0°C. [Adapted, by permission, from Asp L E, Sjogren B A, Berglund L A, *Polym. Composites*, **18**, No.1, 1997, 9-15.]

when carbon black was distributed equally in two phases the fatigue life was 30% better than when all of the carbon black resided in only one phase. Also, uniform distribution of carbon black increased failure resistance.

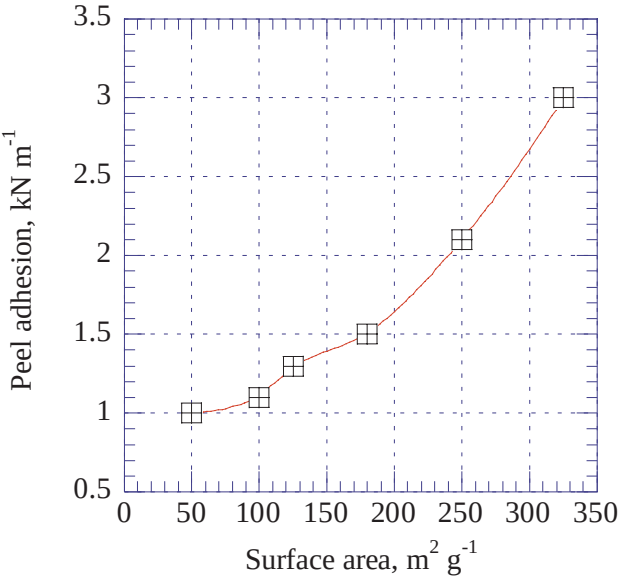

Figure 8.53. Effect of fumed silica surface area on peel adhesion of silicone sealant. [Data from Cochrane H, Lin C-S, *Rubber World*, 1985.]

8.16 ADHESION

This section presents the available data on adhesion of plastic to other substrates in relationship to the concentration of filler.[1,45,77,105,164-5,183-200] Adhesion between filler and the matrix has been discussed in other sections. Figure 8.53 shows the effect of fumed silica on adhesion of silicone sealant. This might be application specific since the adhesion of a silicone sealants is improved by silanes. The increased surface area of fumed silica is associated with an increased concentration of functional groups on its surface, so the improvement is related to the effect of the silane rather than that of the filler.[200]

In another specific application that of hot melt adhesives, the choice of filler has an effect on adhesion (Figure 8.54).[199] Four types of spheres (K-20, S-22, Z-light, and ML 3050) increase adhesion compared with unfilled adhesive. The first two (K-20 and S-22) are hollow microspheres of very low density. The remaining two have a lower density than glass but have thicker walls. Three fillers ($CaCO_3$, Zeospheres, and aluminum) are solid products. All fillers which decrease adhesion have substantially higher thermal conductivity than the fillers which increase adhesion. From the studies of crystallization profiles, it is apparent that longer crystallization times allow the network to orient itself on the substrate, resulting in better adhesion.[199]

In TiO_2 filled coatings either using different amounts of TiO_2 or using TiO_2 with a variety of surface treatments no substantial difference in adhesion was

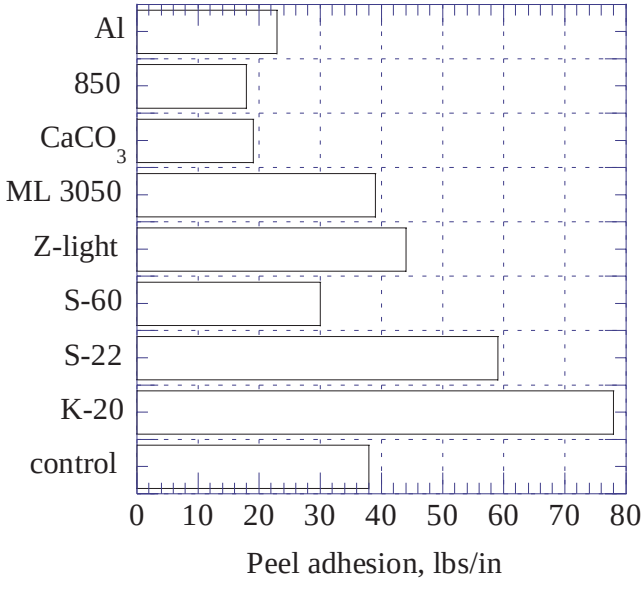

Figure 8.54. Effect of filler type on adhesion of polyurethane adhesive. [Adapted, by permission, from Oien H T, Polyurethanes '95. Conference Proceedings, Chicago, Il., 26th-29th Sept.1995, 137-41.]

found.[185,191] Figure 7.16 indicates that the orientation of polymer on the substrate's surface is responsible for excluding most of the filler from the layer adjacent to the substrate.

The adhesion of PVAc adhesive was improved by the addition of calcite, alumino-silicate and starch but gains were rather small and the mode of failure was altered from cohesive failure in the unfilled sample to adhesive failures in the filled samples.[45]

In PET films containing $CaCO_3$, the adhesion of the film was less than that of unfilled film. This is due to the replacement of the adhesion promoting surface by filler which has no adhesive properties.[197] In UV cured adhesives, quartz filler contributed to a faster development of adhesion due to its transparency to the UV radiation used for curing.[198] In polymer blends filler was accumulated at the interphase between polymers. Adhesion depended on the interaction of filler with both polymers and on the particle size of filler.[188]

In general, fillers may increase the adhesion of plastics to other materials if they can become involved in the mechanism of adhesion (e.g., participate in coupling), change the properties or the orientation of the polymer (e.g., influence curing, elastomeric properties, orientation, etc.). But in many instances fillers may decrease adhesion if they are concentrated at the interface or increase the modulus (higher stress at the interface) of materials or increase viscosity (retarded wetting).

The addition of filler to the material which is combined with other substrates by intermediate layer (adhesive), usually improves adhesion. The adhesion of

LDPE coating to polyester film, clay-coated liner board, and aluminum foil was improved by an addition of calcium carbonate. Adhesion increases as the amount of calcium carbonate is increased and at a 30% level it is doubled.[189] The adhesion of SBR to a polyurethane adhesive was substantially improved (400%) by the addition of silica but only when the surface was roughened. The amount of silica did not affect adhesion of unroughened SBR.[195] The use of MgO with silane coupling increased adhesion of bromobutyl liner by a factor of four.[190] Generally, in the reported data, surface roughening of the filled composite contributes to a better adhesion to other substrates joined by adhesives.

8.17 THERMAL DEFORMATION

Heat distortion temperature is one important property of plastic materials which can be improved by the incorporation of filler.[12-3,20,23-4,43,74] Table 8.4 shows what can be obtained with various systems.

Table 8.4 shows that substantial gains can be obtained by filling crystalline polymers but amorphous polymers are not much affected by reinforcement. Also, particulate fillers are substantially less effective than fibrous fillers. Glass fiber is the most useful filler in this application. Figure 8.55 shows the effect of two grades of particulate fillers on the heat deflection temperature of polypropylene.[43] Small changes are observed at smaller additions followed by a rapid increase in HDT above a 30% filler content. The particle size has only small difference.

8.18 SHRINKAGE

There are several reports on the influence of fillers on shrinkage.[9,115,193,198,201-4] Figure 8.56 shows mold shrinkage vs. concentration of filler.[9] Mold shrinkage can be reduced to half of the value for unfilled resin by the incorporation of mica. Additional reduction of shrinkage is possible if the interaction between filler and the matrix can be increased. This can be achieved by reacting polypropylene with maleic anhydride.[9]

Mold shrinkage is even more efficiently reduced by glass fiber or combination of mica and glass fiber. Glass fiber alone reduces mold shrinkage more effectively than mica. For example, mold shrinkage of in this experiment[201] was 0.28% for 40% glass fiber in polypropylene and 0.96% for 40% mica. If combination of mold shrinkage with warpage reduction is required combination of mica with glass fiber gives better results than the use of glass fiber alone but in such compositions shrinkage increases with mica concentration increasing.[201]

Figure 8.57 shows the anisotropy of mold shrinkage.[202] Unfilled polypropylene (RTP100) shows very big difference between longitudinal and transverse shrinkage. Polypropylene containing 40% calcium carbonate has very similar shrinkage in both directions. In addition, the shrinkage of filled material is consistently lower and less dependent on cycle time. Lower holding times can be used with filled material.[202]

Table 8.4. Heat deflection temperature of various systems

Polymer	Filler	Amount, %	HDT, °C @ 18.6	Ref.
ABS	- glass fiber	0 30	172 358	12
Polyamide-6	- glass fiber	0 30	75 212	12
Polyamide-66	- glass fiber wollastonite	0 30 20	95 248 247	12 13
Polyketone	- glass fiber mica wollastonite $CaCO_3$	0 20 20 20 20	105 210 165 120 95	23
Polyetheretherketone	- glass fiber	0 30	155 315	12
Polybutyleneterephthalate	- glass fiber	0 30	65 210	12
Polypropylene	- glass fiber carbon black talc $CaCO_3$ aluminosilicate	0 30 30 40 40 50	65 148 130 135 116 120	12 74 20 20 43
Polyethersulfone	- glass fiber	0 30	201 216	12
Polyphenylenesulfone	- glass fiber	0 30	172 181	12
Polyarylate	- glass fiber	0 30	175 180	12
Polyimide	- glass fiber	0 30	275 348	12
Polyamide-imide	- glass fiber	0 30	270 275	12
Polyetherimide	- glass fiber	0 30	200 210	12

Proper choice of filler allows to modify shrinkage of UV curable transparent adhesives.[198] The shrinkage of UV curable adhesive was reduced by factor 2-3 by incorporation of quartz which has better UV light transparency than conventionally

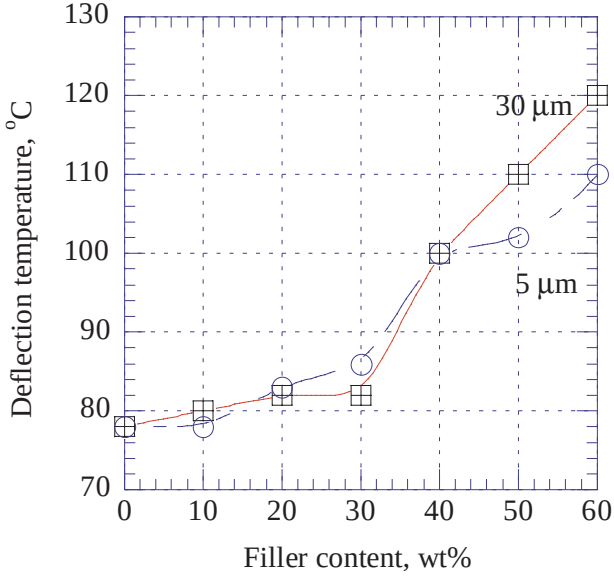

Figure 8.55. Heat deflection temperature of polypropylene containing hydrated K-Mg aluminosilicate. [Adapted, by permission, from Schott N R, Rahman M, Perez M A, *J. Vinyl and Additive Technol*., **1**, No.1, 1995, 36-40.]

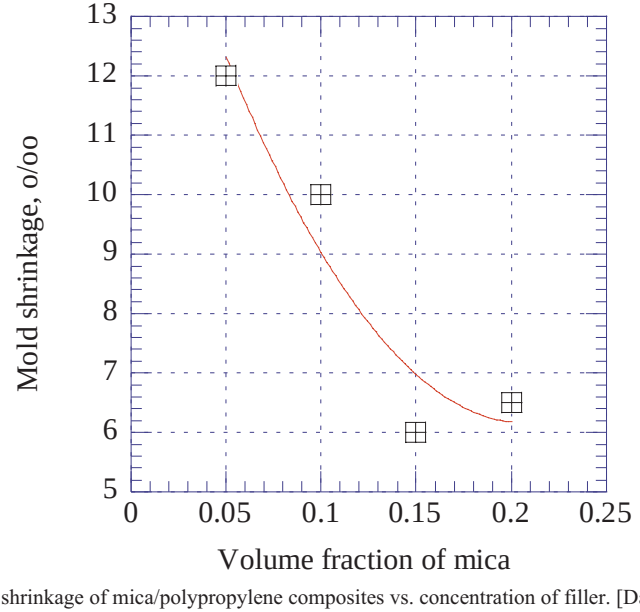

Figure 8.56. Mold shrinkage of mica/polypropylene composites vs. concentration of filler. [Data from Chiang W Y, Yang W D, Pukanszky B, *Polym. Engng. Sci*., **34**, No.6, 1994, 485-92.]

used fillers. Due to more uniform curing and development of network less shrinkage was observed.

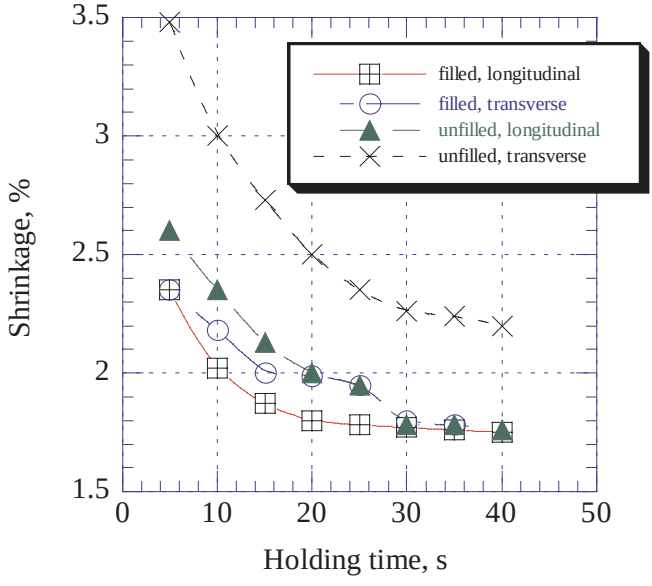

Figure 8.57. Mold shrinkage vs. holding time. [Data from Mamat A, Trochu F, Sanschagrin B, *Polym. Engng. Sci.*, **35**, No.19, 1995, 1511-20.]

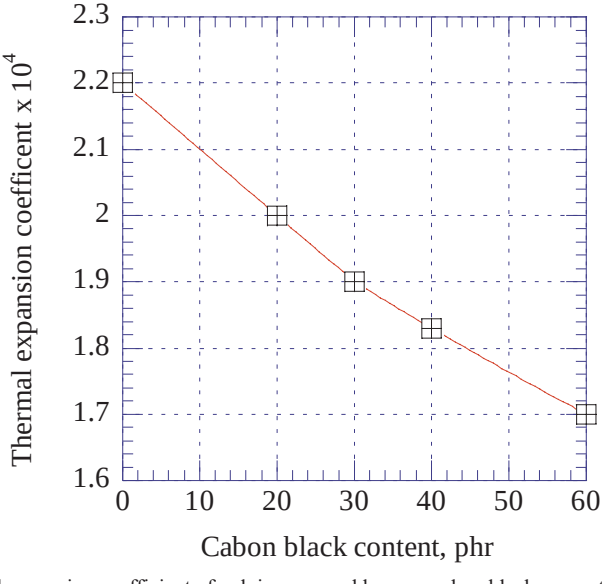

Figure 8.58. Thermal expansion coefficient of polyisoprene rubber vs. carbon black amount. [Data from Priss L S, *Int. Polym. Sci. Technol.*, **23**, No.7, 1996, T53-6.]

Figure 8.58 shows the effect of carbon black on thermal expansion coefficient of rubber.[204] Increasing rubber content contributes to a decrease of thermal expansion.

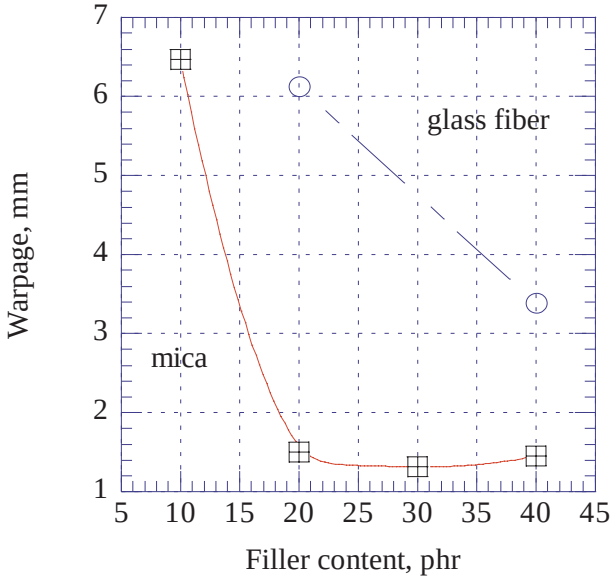

Figure 8.59. Warpage vs. filler content in polypropylene. [Data from Canova L A, Fergusson L W, Parrinello L M, Subramanian R, Giles H F, Antec '97. Conference proceedings, Toronto, April 1997, 2112-6.]

8.19 WARPAGE

Warpage results from residual stresses within a molded part. The ejected part is not constrained by the mold and, if its residual stresses are higher than the modulus of the material, material distortion occurs.[201,205-6] Some fillers can help to decrease warpage.

Figure 8.59 shows the difference in warpage between mica filled and glass fiber filled polypropylene.[201] An increase of mica concentration to 20% is sufficient for a substantial reduction in warpage. Glass fiber can also reduce warpage but it is much less effective than mica. Glass fiber is very efficient in shrinkage reduction (see previous section), so combinations of mica and glass fiber usually give a good balance of properties. In this experiment, the best compromise between shrinkage and warpage was attained when the polypropylene was filled with 20% mica and 20% glass fiber.[201]

Warpage is a function of stress distribution within the material. Stress distribution depends, in turn, on the distribution of filler particles. If filler distribution is not uniform (see section 7.2) stress distribution will vary in different sections of the part. Typically, warpage close to the edges has a different direction of deflection than in the center of the part. Also, there is a higher negative deflection in the region of the part remote from the injection nozzle because these regions are filler deficient.

The type of filler plays an important role. Fillers which have a platelike structure are more efficient than fibers, and fibers are more efficient then particulates.

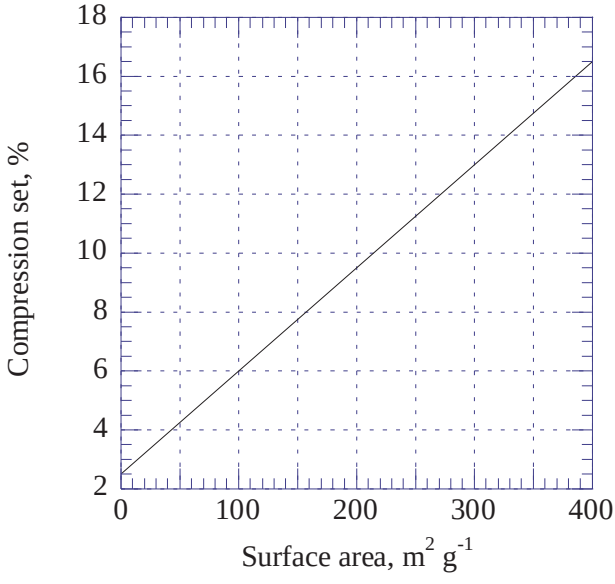

Figure 8.60. Compression set of vulcanized silicone rubber vs. surface area of silica. [Data from Okel T A, Waddell W H, *Rubb. Chem. Technol*., **68**, No.1, 1995, 59-76.]

Orientation of filler particles is also important therefore warpage is influenced by processing conditions which tend to orient the filler such as rate of flow, temperature, ejection temperature, and material crystallization conditions. The current literature does not provide much information on this subject.

8.20 COMPRESSION SET

Compression set is an important property of elastomers which is affected by the choice of filler.[18,121,125,207-9] Studies were conducted on silica in silicon rubber vulcanizates. Figure 8.60 shows the relationship between the surface area of silica and compression set.[125] As the surface area increases compression set increases. The increase surface area contributes to an increase in the number of functional groups on the surface of silica. These groups can potentially react with siloxane. When they do, there is a good interaction of filler with matrix which contributes to reduction of compression set (Figure 8.61).[125]

Acidic silica has more active hydroxyl groups on its surface which increase reactivity. The amount of moisture in silica also increases compression set. This is because promoting its water is necessary to initiate reaction with siloxane and thus its condensation with hydroxyl groups on the surface of silica.

Figure 8.62 shows the compression set of rubber with different fillers at 1:1 proportion to rubber.[207] Fillers, such as precipitated calcium carbonate, whiting, calcinated clay, each of which have limited interaction with the matrix give a substantially lower compression set. As the interaction between filler and the matrix

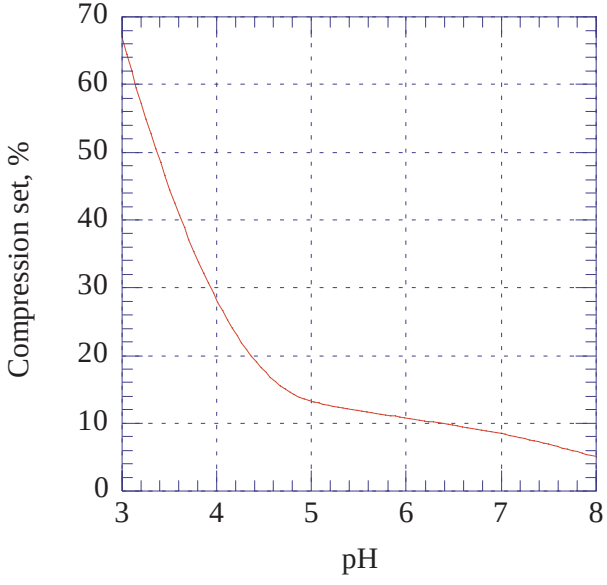

Figure 8.61. Compression stress of vulcanized silicone rubber vs. pH of silica. [Adapted, by permission, from Okel T A, Waddell W H, *Rubb. Chem. Technol*., **68**, No.1, 1995, 59-76.]

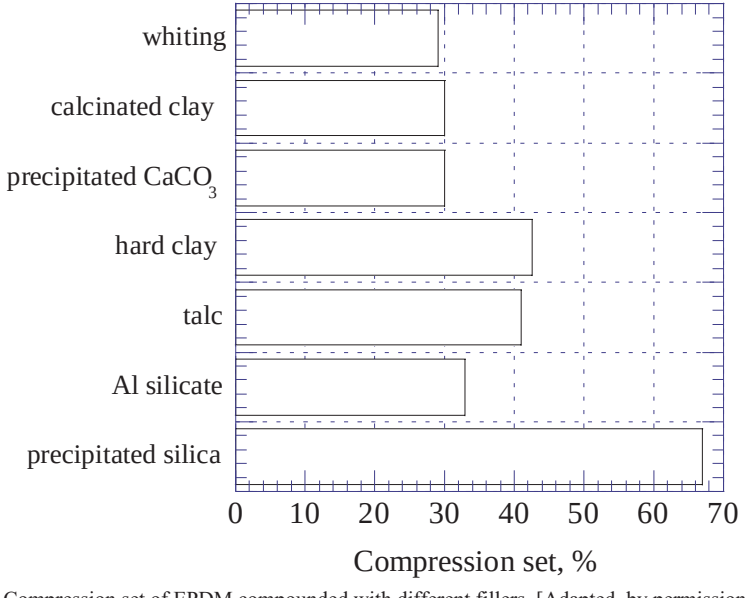

Figure 8.62. Compression set of EPDM compounded with different fillers. [Adapted, by permission, from Mushack R, Luttich R, Bachmann W, *Eur. Rubb. J.*, **178**, No.7, 1996, 24-9.]

increases, compression set increases. This is also found with different grades of silica.[125]

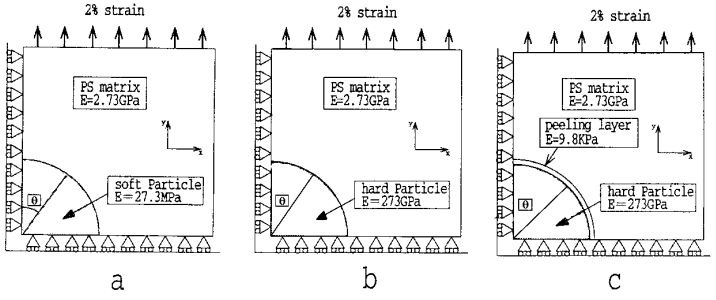

Figure 8.63. Finite element method stress analysis around the particulate in polystyrene. (a) the system with dispersed softer particles, (b) the system with dispersed harder particles, (c) the system with dispersed particles having a peeling layer (adsorbed polymer). [Adapted, by permission, from Mitsui S, Kihara H, Yoshimi S, Okamoto Y, *Polym. Engng. Sci*., **36**, No.17, 1996, 2241-6.]

Cellulose fibers in NBR were found to increase compression set as the concentration of fiber was increased which is consistent with the fact that cellulose interacts with the matrix and increases tensile strength, modulus and abrasion resistance.[18] A comparison of two grades of carbon black shows that one grade decreases compression set in 5 different rubbers whereas the other grade does not change compression set in a broad range of concentrations.[121] The reasons for this are not explained.

8.21 LOAD TRANSFER

This section discusses the structural contribution that fillers make by their participation in stress transfer in filled systems.[5,67,73,90,110,175,204,210-213] The intensity of stress at high concentration of particles (interacting stress fields) is given by:

$$\sigma^* = \frac{\sigma^e}{1 + m\phi^{1/3}} \qquad [8.25]$$

where:

σ^e	external load
m	proportionality constant
ϕ	filler volume concentration

An increased concentration of filler decreases stress around individual particles. Figure 8.63 shows the diagrams used for stress analysis by the finite element method.[110] Figure 8.64 shows the stress concentration factor, C(θ) vs. the angle of the maximum stress concentration point, θ.[110] Soft particles and particles with a peeling layer have a maximum stress concentration at $\theta = 90^o$. This explains why delamination occurs at the poles, perpendicular to the applied strain. The peeling layer forms in the strain direction and crazes propagate from the peeling layer perpendicular to the applied strain.[110]

Stress distribution and load transfer can be conveniently measured by two methods: Raman spectroscopy[210] and NMR.[212] Figure 8.65 shows that the Raman frequency correlates well with the applied strain.[210] The Raman absorption peak

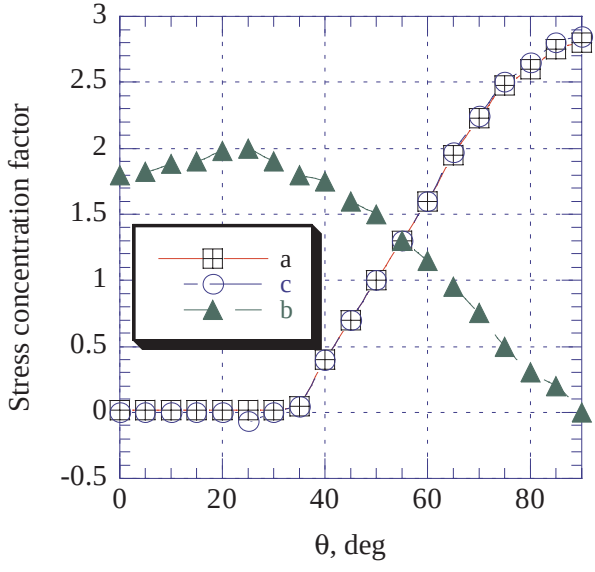

Figure 8.64. Concentration coefficient of the maximum principal stress vs. the highest stress concentration point. Particles types are labeled as in Figure 8.63. [Adapted, by permission, from Mitsui S, Kihara H, Yoshimi S, Okamoto Y, *Polym. Engng. Sci*., **36**, No.17, 1996, 2241-6.]

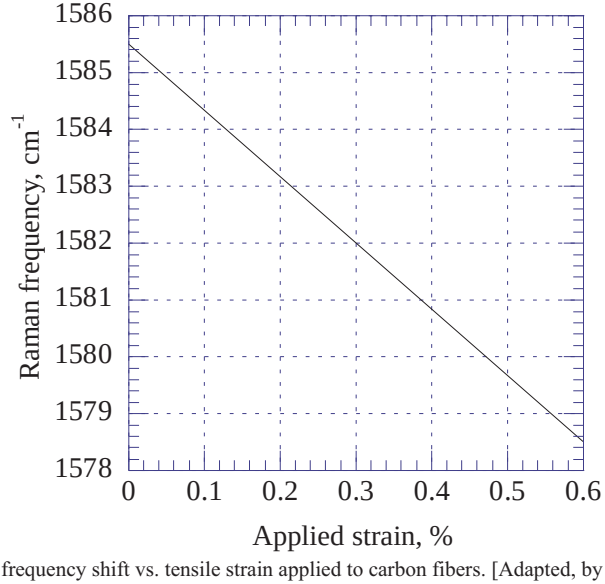

Figure 8.65. Raman frequency shift vs. tensile strain applied to carbon fibers. [Adapted, by permission, from Leveque D, Auvray M H, *Composites Sci. & Technol*., **56**, No.7, 1996, 749-54.]

shifts relative to the applied tensile strain. From this data it is possible to obtain information on elastic load transfer and debonded part. NMR imaging,[212] can be used to calculate the strain map based on measurements of the relaxation time, T_2.

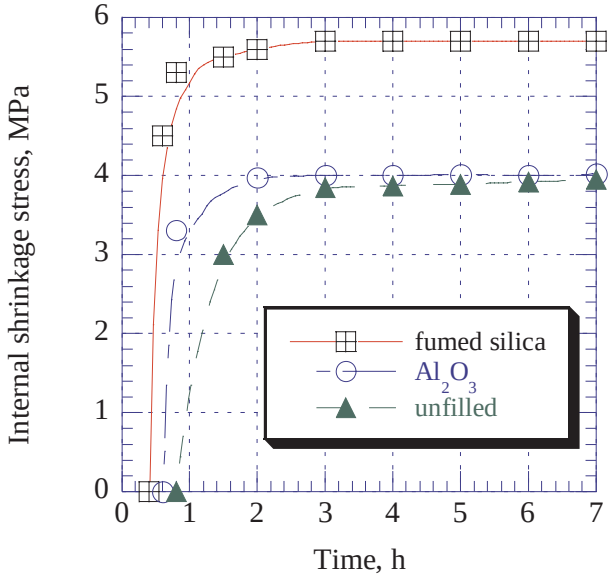

Figure 8.66. Internal shrinkage stress vs. interpenetrating network formation time for PU/PEA=10/90 network. (1) unfilled network, (2) alumina-filled, (3) fumed silica-filled. [Data from Sergeeva L M, Skiba S I, Karabanova L V, Polym. Int., 39, No.4, April 1996, 317-25.]

8.22 RESIDUAL STRESS

The residual stress is associated with changes of volume during processing (cooling, evaporation, crystallization) and during the useful lifetime of the finished products (temperature differences combined with differences in the thermal expansion coefficients of the various materials in formulation). The effect of filler can be predicted.[193,203,210,214] The residual thermal strain was determined in carbon fiber composites by Raman spectroscopy.[210] This stress was not large (-0.1%) but it was concentrated at the fiber ends.

In sheet molded laminates, residual stress decreased as the fiber fraction increased and as the angle of bundle orientation decreased.[214] An increased load can reduce stress as the stresses are distributed throughout the laminate (more interacting surfaces). When the stress is high enough to equal matrix strength, it can cause damage to the laminate. Balancing of stress is a convenient method of improving properties of fiber laminates.

Figure 8.66 shows the effect of different fillers on the residual stress in an interpenetrating network.[203] The stress is determined by the chemical nature of filler. Filler which has a good interaction with the network (such as fumed silica) increases shrinkage stress.

In paints, shrinkage stress influences paint quality. Paint may undergo mud cracking rather than forming a uniform film. Cracking is associated with critical volume packing. If the concentration of filler is higher than critical volume pack-

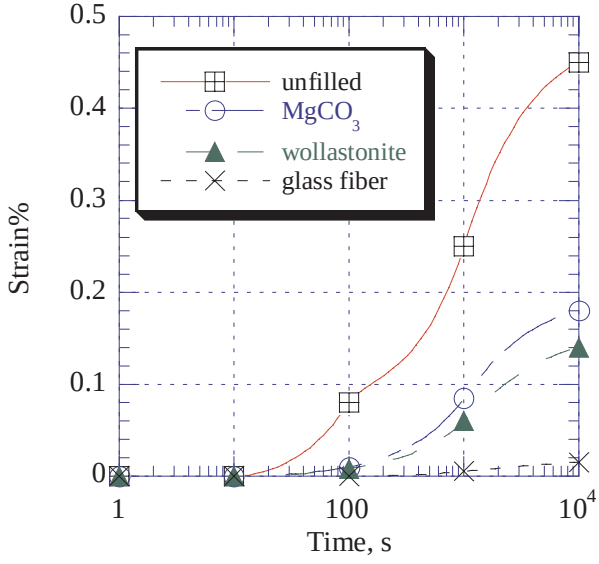

Figure 8.67. Creep strain of LCP vs. time for different fillers. [Adapted, by permission, from Scaffaro R, Pedretti U, La Mantia F P, *Eur. Polym. J.*, **32**, No.7, 1996, 869-75.]

ing, filler particles cannot move closer together and cracking is very likely to occur. The film forming properties of binder also influence shrinkage stress and cracking.[193]

8.23 CREEP

The creep resistance of materials depends on filler-matrix interaction and, therefore, is very much related to fillers use.[7,29,215-7] A simple equation shows creep strain:

$$\frac{\varepsilon_c(t)}{\varepsilon_m(t)} = \frac{E_m}{E_c} \qquad [8.26]$$

where

ε_c	strain of filled polymer
ε_m	strain of matrix (unfilled polymer)
t	time
E_m	Young's modulus of matrix
E_c	Young's modulus of filled polymer

This equation shows that if the creep strain is lower than that predicted by the equation, filler particles induce stress in the surrounding matrix (if no debonding occurs). Figure 8.67 shows the effect of different fillers on creep and Figure 8.68 shows the effect of filler concentration.[29] Creep strain decreases when the filler interaction with matrix increases. This is demonstrated in experiments which show that magnesium carbonate gives a higher strain than does wollastonite and glass fiber. The increased concentration of filler decreases strain. Both results are consistent with the effect of fillers on Young's modulus.

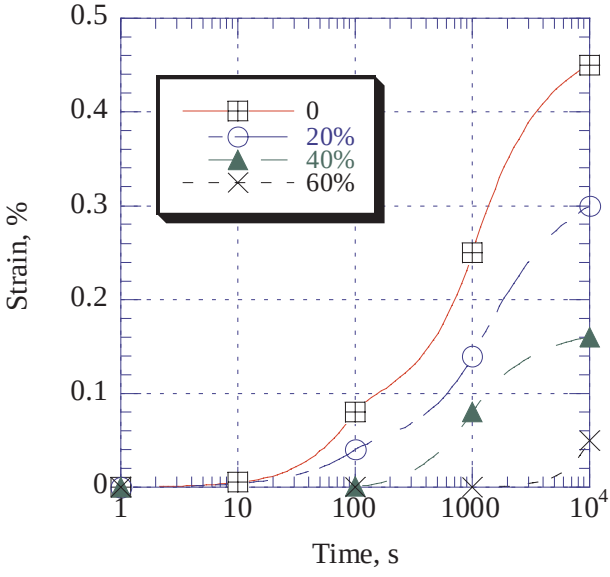

Figure 8.68. Creep strain of LCP vs. time for different concentrations of magnesium carbonate. [Adapted, by permission, from Scaffaro R, Pedretti U, La Mantia F P, *Eur. Polym. J.*, **32**, No.7, 1996, 869-75.]

It was demonstrated that the effect of filler can be fully utilized when stress has sufficient value. At low stress, all glass bead filled composites had the same creep. When stress was increased, it became apparent that surface treatment with different coupling agents produced materials with different creep characteristics. The best results were obtained when glass beads were treated with a combination of silane and bismaleimide. It was also discovered that the creep damage areas appear in the polar regions, in a manner similar to short-term stress-induced damage. After initial debonding microcracks occur at the end of the debonding zone and lead to failure.[215]

The addition of a small amount of glass fiber (7%) to recycled PE and PP drastically reduced creep. This combination was found useful for production of packaging materials from recycled milk bottles.

REFERENCES

1 Kovacevic V, Lucic S, Hace D, Cerovecki Z, *J. Adhesion Sci. Technol.*, **10**, No.12, 1996, 1273-85.
2 Sombatsompop N, Sims G L A, *Cell. Polym.*, **15**, No.5, 1996, 317-34.
3 Zaini M J, Fuad M Y A, Ismail Z, Mansor M S, Mustafah J, *Polym. Int.*, **40**, No.1, 1996, 51-5.
4 Hashemi S, Din K J, Low P, *Polym. Engng. Sci.*, **36**, No.13, 1996, 1807-20.
5 Pukanszky B, Voros G, *Polym.Composites*, **17**, No.3, 1996, 384-92.
6 Hashemi S, Gilbride M T, Hodgkinson J, *J. Mat. Sci.*, **31**, No.19, 1996, 5017-25.
7 Bush S F, Tonkin J D, Antec '97. Conference proceedings, Toronto, April 1997, 3081-85.
8 Meddad A, Fellahi S, Pinard M, Fisa B, Antec '94. Conference Proceedings, San Francisco, Ca., 1st-5th May 1994, Vol. II, 2284-8.
9 Chiang W Y, Yang W D, Pukanszky B, *Polym. Engng. Sci.*, **34**, No.6, 1994, 485-92.
10 Fu Q, Wang G, Liu C, *Polymer*, **36**, No.12, 1995, 2397-401.

11 Godard P, Bomal Y, Biebuyck J J, *J. Mat. Sci*., **28**, No.24, 1993, 6605-10.
12 Maxwell J, **Plastics in High Temperature Applications**, *Rapra*, Shawbury, 1992.
13 Enhancing Polymers Using Additives and Modifiers, *Rapra*, Shawbury, 1993.
14 Ou Y, Yu Z, Zhu J, Li G, Zhu S, *Chinese J. Polym. Sci.*, **14**, No.2, 1996, 172-82.
15 Saad A L G, Younan A F, *Polym. Degradat. Stabil*., **50**, No.2, 1995, 133-40.
16 Younan A F, Choneim A M, Tawfik A A A, Abd-El-Nour K N, *Polym. Degradat. Stabil*., **49**, No.2, 1995, 215-22.
17 Yang Q, Pritchard G, Phipps M A, Rose R G, *Polym. & Polym. Composites*, **4**, No.4, 1996, 239-46.
18 Vieira A, Nunes R C R, Visconti L L Y, *Polym. Bull*., **36**, No.6, 1996, 759-66.
19 Gill T S, Xanthos M, *J. Vinyl and Additive Technol*., **2**, No.3, 1996, 248-52.
20 Hattori K, Morford S, Delany D T, *J. Vinyl and Additive Technol*., **1**, No.3, 1995. 170-3.
21 Bos M, Van Dam G W, Jongsma T, Bruin P, Pennings A J, *Composite Interfaces*, **3**, No.2, 1995, 169-76.
22 Casenave S, Ait-Kadi A, Brahimi B, Riedl B, Antec '95. Vol. II. Conference Proceedings, Boston, Ma., 7th-11th May 1995, 1438-42.
23 Gingrich R P, Machado J M, Londa M, Proctor M G, Antec '95. Vol. II. Conference Proceedings, Boston, Ma., 7th-11th May 1995, 2345-50.
24 Hojabr S, Boocock J R B, Antec 95. Volume III. Conference proceedings, Boston, Ma., 7th-11th May 1995, 3620-7.
25 Gill T S, Xanthos M, Wirsbo Co., Antec '96. Volume II. Conference proceedings, Indianapolis, 5th-10th May 1996, 1757-61.
26 Belanger B, Sanschagrin B, Fisa B, Antec '96. Volume II. Conference proceedings, Indianapolis, 5th-10th May 1996, 1762-7.
27 Montsinger L V, Antec '96. Volume II. Conference proceedings, Indianapolis, 5th-10th May 1996, 2546-9.
28 Johnson K C, Antec '96. Volume III. Conference proceedings, Indianapolis, 5th-10th May 1996, 3545-9.
29 Scaffaro R, Pedretti U, La Mantia F P, *Eur. Polym. J*., **32**, No.7, 1996, 869-75.
30 Sims G L A, Sombatsompop N, *Cell. Polym.*, **15**, No.2, 1996, 90-104.
31 Akovali G, Dilsiz N, *Polym. Engng. Sci*., **36**, No.8, 1996, 1081-6.
32 Lekatou A, Faidi S E, Lyon S B, Newman R C, *J. Mat. Res*., **11**, No.5, 1996, 1293-304.
33 Liu Z, Gilbert M, *J. Appl. Polym. Sci.*, **59**, No.7, 1996, 1087-98.
34 Kurian T, De P P, Tripathy D K, De S K, Peiffer D G, *J. Appl. Polym. Sci*., **62**, No.10, 1996, 1729-34.
35 Alkan C, Arslan M, Cici M, Kaya M, Aksoy M, *Resources Conserv. & Recycling*, **13**, Nos.3-4, 1995, 147-54.
36 Cochet P, Barruel P, Barriquand L, Grobert J, Bomal Y, Prat E, IRC '93/144th Meeting, Fall 1993. Conference Proceedings, Orlando, Fl., 26th-29th Oct.1993, Paper 162.
37 Zaborski M, Slusarski L, Vidal A, *Polim. Tworz. Wielk*., **38**, No.6, 1993, 263-8.
38 Rockenbauer A, Korecz L, Pukanszky B, *Polym. Bull*., **33**, No.5, 1994, 585-9.
39 Ulkem I, Bataille P, Schreiber H P, *J. Macromol. Sci. A*, **31**, No.3, 1994, 291-303.
40 Anantharaman M R, Kurian P, Banerjee B, Mohamed E M, George M, *Kaut. u. Gummi Kunst.*, **49**, No.6, 1996, 424-6.
41 Schneider J P, Myers G E, Clemons C M, English B W, *J. Vinyl and Additive Technol*., **1**, No.2, 1995, 103-8.
42 Zolotnitsky M, Steinmetz J R, *J. Vinyl and Additive Technol*., **1**, No.2, 1995, 109-13.
43 Schott N R, Rahman M, Perez M A, *J. Vinyl and Additive Technol*., **1**, No.1, 1995, 36-40.
44 Clemens M L, Doyle M D, Lees G C, Briggs C C, Day R C, Flame Retardants '94. Conference proceedings, London, 27th-28th January 1994, 193-202.
45 Kovacevic V, Lucic S, Hace D, Glasnovic A, Smit I, Bravar M, *J. Adhesion*, **47**, No.1-3, 1994, 201-15.
46 Pechulis M, Vautour D, Antec '97. Conference proceedings, Toronto, April 1997, 1860-4.
47 Barbosa S E, Kenny J M, Antec '97. Conference proceedings, Toronto, April 1997, 1855-9.
48 Davis R M, Gardner S H, Marand E, Laot C, Reifsnider K, DeSmidt H, McGrath J, Tan B, Antec '97. Conference proceedings, Toronto, April 1997, 2494-9.
49 Kumar P, Gawahale A R, Rai B, *Adv. Composite Materials*, **4**, No.4, 1995, 279-85.
50 Canova L A, Antec '93. Conference Proceedings, New Orleans, La., 9th-13th May 1993, Vol. II, 1943-9.
51 Liptak P, *Int. Polym. Sci. Technol*., **21**, No.8, 1994, T/50-3.
52 Sato T, *Int. Polym. Sci. Technol*., **21**, No.3, 1994, T/45-52.

53 Pukanszky B, Belina K, Rockenbauer A, Maurer F H J, *Composites*, **25**, No.3, 1994, 205-14.
54 Byung Suk Jin, Kwang Hee Lee, Chul Rim Choe, *Polym. Int*., **34**, No.2, 1994, 181-5.
55 Bataille P, Mahlous M, Schreiber H P, *Polym. Engng. Sci*., **34**, No.12, 1994, 981-5.
56 Lan T, Pinnavaia T J, *Chem. of Mat*., **6**, No.12, 1994, 2216-9.
57 Nicolais L, Narkis M, *Polym. Eng. Sci*., **11**, 1971, 194.
58 Nielsen L E, *J. Appl. Phys*., **4**, 1970, 4626.
59 Piggott M R, Leidner J, *J. Appl. Polym. Sci.,* **18**, 1974, 1619.
60 Kelly A, Tyson W R, *J. Mech. Phys. Solids*, **6**, 1965, 13.
61 Yamada H, Inagaki S, Okamoto H, Furukawa J, *Int. Polym. Sci. Technol*., **21**, No.6, 1994, T/29-35.
62 Enhancing Polymers Using Additives and Modifiers II, *Rapra*, Shawbury, 1996, paper 5.
63 Miller B, *Plast. World*, **54**, No.1, 1996, 38-43.
64 Hornsby P R, Watson C L, *J. Mat. Sci*., **30**, No.21, 1995, 5347-55.
65 Cochrane H, Lin C S, *Rubb. Chem. Technol*., **66**, No.1, 1993, 48-60.
66 Bhattacharya S K, Bhowmick A K, Singh R K, *J. Mat. Sci*., **30**, No.1, 1995, 243-7.
67 Voros G, Pukanszky, *J. Mat. Sci*., **30**, No.16, 1995, 4171-8.
68 Cheung T, Tjong S C, Li R K Y,Antec '96. Volume II. Conference proceedings, Indianapolis, 5th-10th May 1996, 2256-9.
69 Liu Z, Gilbert M, *J. Appl. Polym. Sci.*, **59**, No.7, 1996, 1087-98.
70 Wiebking H E, *J. Vinyl and Additive Technol*., **2**, No.3, 1996, 187-9.
71 Wiebking H E, Antec 95. Volume III. Conference proceedings, Boston, Ma., 7th-11th May 1995, 4112-6.
72 Pukanszky B, Maurer F H J, Boode J W, *Polym. Engng. Sci*., **35**, No.24, 1995, 1962-71.
73 Savadori A, Scapin M, Walter R, *Macromol. Symp*., **108**, 1996, 183-202.
74 Chiu H-T, Chiu W-M, *J. Appl. Polym. Sci*., **61**, No.4, 1996, 607-12.
75 Zihlif A M, Di Liello V, Martuscelli E, Ragosta G, *Int. J. Polym. Mat*., **29**, Nos.3-4, 1995, 211-20.
76 Jancar J, Dibenedetto A T, *J. Mat. Sci.*, **30**, No.6, 1995, 1601-8.
77 Jancar J, DiBenedetto A T, *Sci. & Eng. Composite Materials*, **3**, No. 4, 1994, 217-26.
78 Wang M-J, Wolff S, Tan E-H, *Rubb. Chem. Technol*., **66**, No.2, 1993, 178-95.
79 Palumbo M, Donzella G, Tempesti E, Ferruti P, *J. Appl. Polym. Sci*., **60**, No.1, 1996, 47-53.
80 Jancar J, *Macromol. Symp*., **108**, 1996, 163-72.
81 Averous L, Quantin J C, Lafon D, Crespy A, *Int. J. Polym. Analysis and Characterization*, **1**, No.4, 1995, 339-47.
82 Beloshenko V A, Kozlov G V, Slobodina V G, Prut E V, Grinev V G, *Polym. Sci., Ser. B*, **37**, Nos.5-6, 1995, 316-8.
83 Babich V F, Lipatov Yu S, Todosijchuk T T, *J. Adhesion*, **55**, Nos.3-4, 1996, 317-27.
84 Guerrica-Echevarria G, Eguiazabal J I, Nazabal J, *Polym. Degradat. Stabil*., **53**, No.1, 1996, 1-8.
85 Jones D W, Rizkalla A S, *J. Biomedical Materials Research (Applied Biomaterials)*, **33**, No.2, 1996, 89-100.
86 Owen A J, Koller I, *Polymer*, **37**, No.3, 1996, 527-30.
87 Wong K W Y, Truss R W, *Composites Sci. & Technol*., **52**, No.3, 1994, 361-8.
88 Yang A C M, *Polymer*, **35**, No.15, 1994, 3206-11.
89 Roesch J, Barghoorn P, Muelhaupt R, *Makromol. Chem. Rapid Commun*., **15**, No.9, 1994, 691-6.
90 Sjogren B A, Berglund L A, *Polym. Composites*, **18**, No.1, 1997, 1-8.
91 Y. S. Lipatov, **Polymer Reinforcement**, *ChemTec Publishing*, Toronto, 1995.
92 Akay M, Mun S K A, Stanley A, *Composites Sci. Technol,* **57**, 1997, 565-71.
93 Leguet X, Ericson M, Chundury D, Baumer G, Antec '97. Conference proceedings, Toronto, April 1997, 2117-34.
94 Ohta M, Nakamura Y, Hamada H, Maekawa Z, *Polym. & Polym. Composites*, **2**, No.4, 1994, 215-21.
95 Yang Q, Pritchard G, *Polym. & Polym. Composites*, **2**, No.4, 1994, 233-9.
96 Ou Y C, Zhu J, Feng Y P, *J. Appl. Polym. Sci*., **59**, No.2, 1996, 287-94.
97 Gahleitner M, Bernreitner K, Knogler B, Neissl W, *Macromol. Symp*., **108**, 1996, 127-36.
98 Tan L S, McHugh A J, Gulgun M A, Kriven W M, *J. Mat. Res*., **11**, No.7, 1996, 1739-47.
99 Tan L S, McHugh A J, *J. Mater. Sci.*, **31**, 1996, 3701-6.
100 Sanchez-Solis A, Padilla A, *Polym. Bull*., **36**, No.6, 1996, 753-58.
101 Toure B, Lopez Cuesta J-M, Longerey M, Crespy A, *Polym. Degradat. Stabil*., **54**, Nos 2-3, 1996, 345-52.
102 Thomason J L, Vlug M A, *Composites, Part A*, **28A**, 1997, 277-88.
103 Herzig R, Baker W E, *J. Mat. Sci*., **28**, No.24, 1993, 6531-9.

104 Pukanszky B, Maurer F H J, *Polymer*, **36**, No.8, 1995, 1617-25.
105 Jancar J, Dibenedetto A T, Dianselmo A, *Polym. Engng. Sci*., **33**, No.9, 1993, 559-63.
106 Jancar J, DiBenedetto A T, Antec '94. Conference Proceedings, San Francisco, Ca., 1st-5th May 1994, Vol. II, 1710-2.
107 Skelhorn D A, Antec '93. Conference Proceedings, New Orleans, La., 9th-13th May 1993, Vol. II, 1965-70.
108 Plummer C J G, Wu Y, Gola M M, Kausch H H, *Polym. Bull*., **30**, No.5, 1993, 587-94.
109 Nabi Z U, Hashemi S, *J. Mat. Sci*., **31**, No.21, 1996, 5593-601.
110 Mitsui S, Kihara H, Yoshimi S, Okamoto Y, *Polym. Engng. Sci*., **36**, No.17, 1996, 2241-6.
111 Qi Wang, Jizhuang Cao, Guangjin Li, Xi Xu, *Polym. Int*., **41**, No. 3, 1996, 245-9.
112 Tiganis B E, Shanks R A, Long Y, Antec '96. Volume II. Conference proceedings, Indianapolis, 5th-10th May 1996, 1744-9.
113 McIlvaine J, Antec 95. Volume III. Conference proceedings, Boston, Ma., 7th-11th May 1995, 3346-9.
114 Yu M C, Bissell M A, Whitehouse R S, Antec 95. Volume III. Conference proceedings, Boston, Ma., 7th-11th May 1995, 3246-50.
115 Yu T C, Antec '95. Vol. II. Conference Proceedings, Boston, Ma., 7th--11th May 1995, 2358-68.
116 Wang K J, Sue H J, Antec '95. Vol. II. Conference Proceedings, Boston, Ma., 7th-11th May 1995, 1758-64.
117 Yeh J T, Yang H M, Huang S S, *Polym. Degradat .Stabil*., **50**, No.2, 1995, 229-34.
118 Toure B, Lopez Cuesta J M, Gaudon P, Benhassaine A, Crespy A, *Polym. Degradat. Stabil*., **53**, No.3, 1996, 371-9.
119 Vasnev V A, Tarasov A I, Istratov V N, Ignatov V N, Krasnov A P, Kuznetsov A I, Surkova I N,Russia, *Reactive & Functional Polym.*, **26**, Nos.1-3, 1995, 177-83.
120 Evans L R, Meeting of the Rubber Division, ACS, Montreal, May 5-8, 1996, paper D.
121 Monthey S, Duddleston B, Podobnik J, *Rubb. World*, **210**, No.3, 1994, 17-9.
122 Abdel-Aziz M M, Gwaily S E, *Polym. Degradat. Stabil*., **55**, 1997, 269-74.
123 Kurian T, De P P, Khastgir D, Tripathy D K, De S K, Peiffer D G, *Polymer*, **36**, No.20, 1995, 3875-84.
124 Kim S G, Lee S H, *Rubb. Chem. Technol*., **67**, No.4, 1994, 649-61.
125 Okel T A, Waddell W H, *Rubb. Chem. Technol*., **68**, No.1, 1995, 59-76.
126 Ismail H, Freakley P K, Sutherland I, Sheng E, *Eur. Polym. J*., **31**, No.11, 1995, 1109-17.
127 Ismail H, Freakley P K, Sheng E, *Eur. Polym. J*., **31**, No.11, 1995, 1049-56.
128 Tamura J, Kawanabe K, Yamamuro T, Nakamura T, Kokubo T, Yoshihara S, Shibuya T, *J. Biomed. Mat. Res.*, **29**, No.5, 1995, 551-9.
129 Nofal M M, Zihlif A M, Ragosta G, Martuscelli E, *Polym. Composites*, **17**, No.5, 1996, 705-9.
130 Hornsby P R, Premphet K, *J. Mater. Sci*., **32**, 1997, 4767-75.
131 Qiu Q, Kumosa M, *Composites Sci. Technol,* **57**, 1997, 497-507.
132 Becu L, Maazouz A, Sautereau H, Gerard J F, *J. Appl. Polym. Sci*., **65**, 1997, 2419-31.
133 Li J X, Silverstein M, Hiltner A, Baer E, *J. Appl. Polym. Sci.*, **52**, No.2, 1994, 255-67.
134 Li J X, Hiltner A, Baer E, *J. Appl. Polym. Sci*., **52**, No.2, 1994, 269-83.
135 Ping Gu, Ping Xie, Beaudoin J J, *Cement & Concrete Comp*., **15**, No.3, 1993, 173-80.
136 Dose T M, Antec '97. Conference proceedings, Toronto, April 1997, 3314-8.
137 Okiyokota M, Hamada H, Hiragushi M, Hasegawa T, Antec '97. Conference proceedings, Toronto, April 1997, 3319-21.
138 Donnet J B, *Kaut. u. Gummi Kunst*., **47**, No.9, 1994, 628-32.
139 Khan S A, Baker G L, Colson S, *Chem. of Mat*., **6**, No.12, 1994, 2359-63.
140 Azimi H R, Pearson R A, Hertzberg R W, *J. Appl. Polym. Sci*., **58**, No.2, 1995, 449-63.
141 Yu Long, Shanks R A, *J. Appl. Polym. Sci*., **61**, No.11, 1996, 1877-85.
142 Liu C T, Ravi-Chandar K, J. *Reinf. Plast. Comp*.,**15**, No.2, 1996, 196-207.
143 Bagheri R, Pearson R A, *Polymer*, **36**, No.25, 1995, 4883-5.
144 Seibel S R, Moet A, Bank D H, Sehanobish K, Antec 95. Volume III. Conference proceedings, Boston, Ma., 7th-11th May 1995, 3966-70.
145 Conductive Polymers, *Rapra*, Shawbury, 1992.
146 Fengyuan Yan, Qunji Xue, Shengrong Yang, *J. Appl. Polym. Sci*., **61**, No.7, 1996, 1223-9.
147 Fengyuan Yan, Wenhua Wang, Qunji Xue, Long Wei, *J. Appl. Polym. Sci.*, **61**, No.7, 1996, 1231-6.
148 Shiqi He, Qianchu Liu, Yiu-Wing Mai, Bryant R, *J. Mat. Sci. Mat. In Med*., **7**, No.10, 1996, 611-6.
149 Shin Jen Shiao, Te Zei Wang, *Composites*, **27B**, No.5, 1996, 459-65.
150 Braches E, *Kunststoffe Plast. Europe*, **86**, No.11, 1996, 21-2.
151 Srivastava V K, Pathak J P, *Polym. & Polym. Composites*, **3**, No.6, 1995, 411-4.

152 Zhang C-Z, Liu W-M, Xue Q-J, Shen W-C, *J. Appl. Polym. Sci*., **66**, 1997, 85-93.
153 Wada N, Uchiyama Y, Hosokawa M, *Int. Polym. Sci. Technol*., **21**, No.3, 1994, T/53-63.
154 Wada N, Uchiyama Y, *Int. Polym. Sci. Technol*., **21**, No.10, 1994, T/23-34.
155 Knowles J, *Polym. Paint Col. J.*, **185**, No.4366, 1995, 26-7.
156 Patel A C, *Kaut. u. Gummi Kunst*., **47**, No.8, 1994, 556-70.
157 Bijwe J, *Polym. Composites*, **18**, No.3, 1997, 378-96.
158 Kody R S, Martin D C, *Polym. Engng. Sci*., **36**, No.2, 1996, 298-304.
159 Schmidt H K, *Macromol. Symp*., **101**, 1996, 333-42.
160 Schuster R H, Meeting of the Rubber Division, ACS, Montreal, May 5-8, 1996, paper F.
161 Kontou E, *J. Reinf. Plast. Comp*., **13**, No.8, 1994, 756-66.
162 Horst J J, Spoormaker J L, *J. Mater. Sci*., **32**, 1997, 3641-51.
163 Zhou J, Li G, Li B, He T, *J. Appl. Polym. Sci*., **65**, 1997, 1857-64.
164 Xu X X, Crocrombe A D, Smith P A, *Int. J. Fatigue*, **16**, No.7, 1994, 469-77.
165 Xu X X, Crocombe A D, Smith P A, *Int. J. Fatigue*, **17**, No.4, 1995, 279-86.
166 Seibel S R, Moet A, Bank D H, Nichols K, Antec '93. Conference Proceedings, New Orleans, La., 9th-13th May 1993, Vol. I, 902-5.
167 Jia N, Kagan V A, Antec '97. Conference proceedings, Toronto, April 1997, 1844-8.
168 Topoleski L D T, Ducheyne P, Cuckler J M, *J. Biomed. Mat. Res*., **29**, No.3, 1995, 299-307.
169 Visser S A, *J. Appl. Polym. Sci*., **63**, 1997, 1805-20.
170 Visser S A, *J. Appl. Polym. Sci*., **64**, 1997, 1499-1509.
171 Trotignon J P, Tcharkhtchi A, *Macromol. Symp*., **108**, 1996, 231-45.
172 Dyrda V I, Meshchaninov S K, *Int. Polym. Sci. Technol*., **22**, No.12, 1995, T/14-6.
173 Visser S A, Hewitt C E, Binga T D, *J. Polym. Sci., Polym. Phys*., **34**, No.9, 1996, 1679-89.
174 Gownder M, Letton A, Hogan H,Antec '95. Vol. II. Conference Proceedings, Boston, Ma., 7th-11th May 1995, 1983-6.
175 Asp L E, Sjogren B A, Berglund L A, *Polym. Composites*, **18**, No.1, 1997, 9-15.
176 Cantwell W J, Zulkifli R, *J. Mater. Sci*. *Lett*., **16**, 1997, 509-11.
177 Wang S Q, Inn Y W, *Rheol. Acta*, **33**, No.2, 1994, 108-16.
178 Kominar V, Narkis M, Siegmann A, Breuer O, *Sci. & Engng. Composite Materials*, **3**, No.1, 1994, 61-6.
179 Jancar J, Dibenedetto A T, *J. Mat. Sci*., **30**, No.9, 1995, 2438-45.
180 Rodrigues F, Antec '93. Conference Proceedings, New Orleans, La., 9th-13th May 1993, Vol. I, 332-7.
181 Herd C R, Bomo F, *Kaut. u. Gummi Kunst*., **48**, No.9, 1995, 588-99.
182 Hauser R L, Woods D W, Krause-Singh J, Ferry S R, Antec '93. Conference Proceedings, New Orleans, La., 9th-13th May 1993, Vol. I, 341-6.
183 Vilgis T A, Heinrich G, *Macromolecules*, **27**, No.26, 1994, 7846-54.
184 Gent A N, Lai S-M, *Rubb. Chem. Technol*., **68**, No.1, 1995, 13-25.
185 Hegedus C R, Kamel I L, *J. Coatings Technol*., **65**, No.822, July 1993, 37-43.
186 Zhuk A V, Knunyants N N, Oshmyan V G, *Polym. Sci*., **36**, No.4, 1994, 572-5.
187 Vratsanos L A, Farris R J, *Polym. Engng. Sci*., **33**, No.22, 1993, 1458-65.
188 Kiselev V Ya, *Int. Polym. Sci. Technol*., **21**, No.7, 1994, T/52-5.
189 Ruiz F A, Polymers, Laminations & Coatings Conference, 1995, 647-51.
190 Cochet P, Bomal Y, *Kaut. u. Gummi Kunst*., **48**, No.4, 1995, 270-5.
191 Roche A A, Dole P, Bouzziri M, *J. Adhesion Sci. Technol*., **8**, No.6, 1994, 587-609.
192 Lee I, *J. Mat. Sci*., **30**, No.23, 1995, 6019-22.
193 Hoy L L, *J. Coatings Technol*., **68**, No.853, 1996, 33-9.
194 Kiselev V Y, Vnukova V G, *Int. Polym. Sci. Technol*., **23**, No.5, 1996, T/88-92.
195 Torro-Palau A, Fernandez-Garcia J C, Orgiles-Barcelo A C, Martin-Martinez J M, *J. Adhesion*, **57**, Nos.1-4, 1996, 203-25.
196 Tsutsumi K, Ban K, Shibata K, Okazaki S, Kogoma M, *J. Adhesion*, **57**, Nos.1-4, 1996, 45-53.
197 Casoli A, Charmeau J Y, Holl Y, d'Allest J F, *J. Adhesion*, **57**, Nos.1-4, 1996, 133-51.
198 Murata N, Nishi S, Hosono S, *J. Adhesion*, **59**, Nos.1-4, 1996, 39-50.
199 Oien H T, Polyurethanes '95. Conference Proceedings, Chicago, Il., 26th-29th Sept.1995, 137-41.
200 Cochrane H, Lin C-S, *Rubber World*, 1985.
201 Canova L A, Fergusson L W, Parrinello L M, Subramanian R, Giles H F, Antec '97. Conference proceedings, Toronto, April 1997, 2112-6.
202 Mamat A, Trochu F, Sanschagrin B, *Polym. Engng. Sci*., **35**, No.19, 1995, 1511-20.
203 Sergeeva L M, Skiba S I, Karabanova L V, *Polym. Int*., **39**, No.4, April 1996, 317-25.

204 Priss L S, *Int. Polym. Sci. Technol*., **23**, No.7, 1996, T53-6.
205 Schultz R, Antec '96. Vol. I. Conference Proceedings, Indianapolis, 5th-10th May 1996, 519-24.
206 Heberlein D E, Antec '94. Conference Proceedings, San Francisco, Ca., 1st-5th May 1994, Vol. I, 791-5.
207 Mushack R, Luttich R, Bachmann W, *Eur. Rubb. J.*, **178**, No.7, 1996, 24-9.
208 Lawandy S N, Botros S H, Darwish N A, Mounir A, *Polym. Plast. Technol. Engng*., **34**, No.6, 1995, 861-74.
209 Wang W D, Haidar B, Vidal A, Donnet J B, *Kaut. u. Gummi Kunst*., **47**, No.4, 1994, 238-41.
210 Leveque D, Auvray M H, *Composites Sci. & Technol*., **56**, No.7, 1996, 749-54.
211 Kim G M, Michler G H, Gahleitner M, Fiebig J, *J. Appl. Polym. Sci*., **60**, No.9, 1996, 1391-403.
212 Bluemler P, Bluemich B, *Acta Polymerica*, **44**, No.3, 1993, 125-31.
213 Sinien L, Yongli W, Zhifa D, Yuchun O, Xiaoping F, Antec '96. Volume II. Conference proceedings, Indianapolis, 5th-10th May 1996, 2298-300.
214 Kabelka J, Hoffmann L, Ehrenstein G W, *J. Appl. Polym. Sci*., **62**, No.1, 1996, 181-98.
215 Sinien L, Xiaoguang Z, Zhongneng Q, Huan X, *J. Mat. Sci. Lett*., **14**, No.20, 1995, 1458-60.
216 Simhambhatla M, Leonov A I, *Rheol. Acta*, **34**, No.4, 1995, 329-38.
217 Dufresne A, Lacabanne C, *Polymer*, **34**, No. 15, 1993, 3173-8.